AD-A064 098 ARMY ARMAMENT RESEARCH AND DEVELOPMENT COMMAND ABERD--ETC F/G 7/4
ENERGY TRANSFER IN A 2 SIGMA (+) OH II. VIBRATIONAL.(U)
NOV 78 R K LENGEL, D R CROSLEY

UNCLASSIFIED ARBRL-TR-02118 SBIE-AD-E430 160 NL

1 OF 1
AD A064098

END
DATE FILMED
4-79
DDC

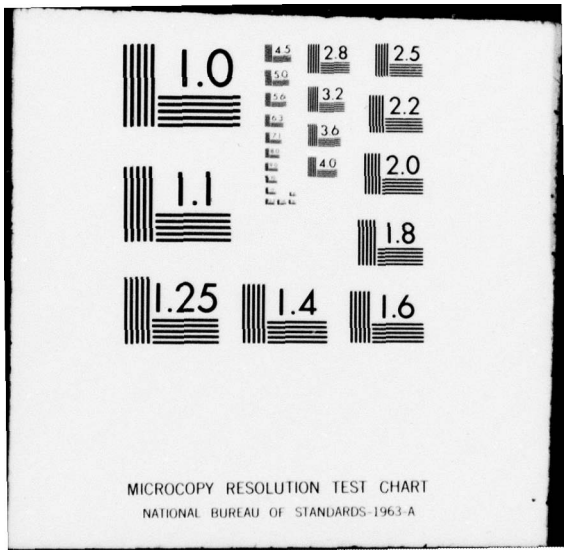
1.0
1.1
1.25
1.4
1.6
1.8
2.0
2.2
2.5
2.8
3.2
3.6
4.0
4.5
5.0
5.6
MICROCOPY RESOLUTION TEST CHART
NATIONAL BUREAU OF STANDARDS-1963-A

(12) LEVEL II

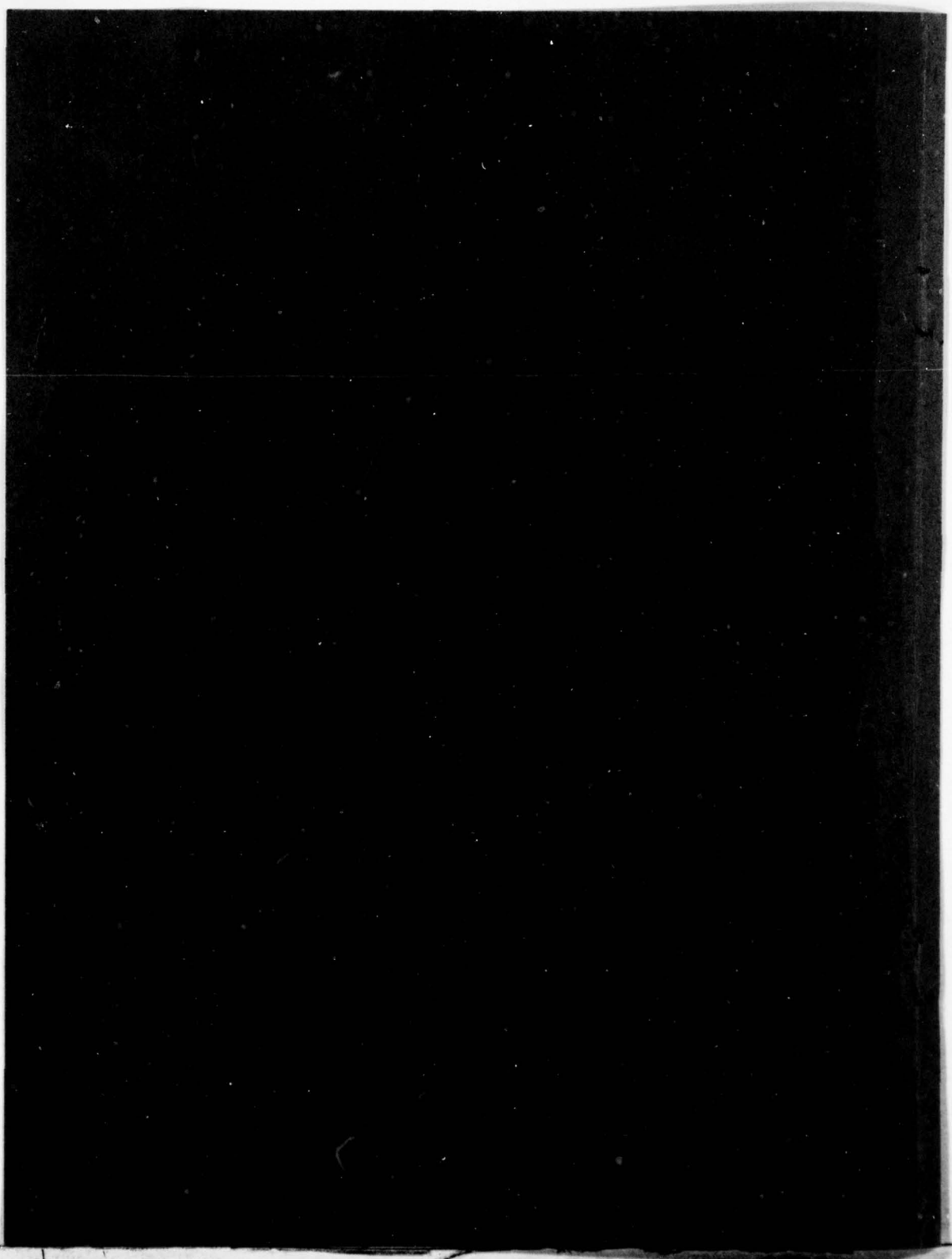

UNCLASSIFIED

SECURITY CLASSIFICATION OF THIS PAGE (When Data Entered)

REPORT DOCUMENTATION PAGE

READ INSTRUCTIONS BEFORE COMPLETING FORM

1. REPORT NUMBER: TECHNICAL REPORT ARBRL-TR-02118
2. GOVT ACCESSION NO.
3. RECIPIENT'S CATALOG NUMBER: (9) Technical rept.

4. TITLE (and Subtitle): (6) ENERGY TRANSFER IN $A^2\Sigma^+$ OH A 2 Sigma (+) OH
II. VIBRATIONAL
5. TYPE OF REPORT & PERIOD COVERED
6. PERFORMING ORG. REPORT NUMBER

7. AUTHOR(s): (10) Russell K. Lengel* David R. Crosley
8. CONTRACT OR GRANT NUMBER(s)

9. PERFORMING ORGANIZATION NAME AND ADDRESS:
US Army Ballistic Research Laboratory
(ATTN: DRDAR-BLB)
Aberdeen Proving Ground, MD 21005
10. PROGRAM ELEMENT, PROJECT, TASK AREA & WORK UNIT NUMBERS: (16) RDT&E 1L161102AH43

11. CONTROLLING OFFICE NAME AND ADDRESS:
US Army Armament Research and Development Command
US Army Ballistic Research Laboratory
(ATTN: DRDAR-BL)
Aberdeen Proving Ground, MD 21005
12. REPORT DATE: NOV 1978
13. NUMBER OF PAGES: 77

14. MONITORING AGENCY NAME & ADDRESS (if different from Controlling Office): (12) 73p.
15. SECURITY CLASS. (of this report): Unclassified
15a. DECLASSIFICATION/DOWNGRADING SCHEDULE

16. DISTRIBUTION STATEMENT (of this Report)

Approved for public release; distribution unlimited.

(18) SBIE (19) AD-E430 160

17. DISTRIBUTION STATEMENT (of the abstract entered in Block 20, if different from Report)

DDC RECEIVED FEB 2 1979 B

18. SUPPLEMENTARY NOTES

*Department of Chemistry, University of Wisconsin

19. KEY WORDS (Continue on reverse side if necessary and identify by block number)
Energy Transfer
Vibrational Relaxation
OH Molecule
State-to-State Transfer
Laser Excited Fluorescence

20. ABSTRACT (Continue on reverse side if necessary and identify by block number) (eal)

Vibrational energy transfer within the A state of OH and OD has been studied. A frequency doubled tunable dye laser excites individual N', J' levels in v'=1 or 2, and the intensities of rotationally resolved fluorescence emitted in the presence of collision partners (helium, argon hydrogen, deuterium and nitrogen) furnishes state-to-state transfer rates. It is found that the transfer rates are strongly dependent on initial rotational level (decreasing as the rotational quantum number increases), that the final rotational state (CONTD)

DD FORM 1 JAN 73 1473 EDITION OF 1 NOV 65 IS OBSOLETE

78 12 06 016

UNCLASSIFIED

SECURITY CLASSIFICATION OF THIS PAGE (When Data Entered)

393 471

distributions are near thermal but hot, that isoenergetic transfer is small, and that the magnitudes for transfer 1→0, 2→0 are all similar. The rates themselves are large; for example, with nitrogen the cross section for 1→0 transfer with N=3 is 21 square Angstrom. The results, taken together, are supportive of a long-lived collision in which anisotropic attractive forces are of importance in the dynamics of the entrance channel.

TABLE OF CONTENTS

LIST OF ILLUSTRATIONS

LIST OF TABLES

INTRODUCTION

Due to progress and innovations in experimental technique, particularly the increasing use of lasers, a good deal of attention has been directed recently toward the study of molecular collisions on a state-resolved basis.[1] The state of the art remains far from that penultimate experiment, a full internal state resolution of both reactants and products, including specification and measurement of velocities and scattering angles. Nonetheless a number of instances have been found which exhibit a detailed (and occasionally surprising) quantum level dependence of various collision processes, and some theoretical overviews are beginning to emerge.

We have studied energy transfer processes occurring within the $A^2\Sigma^+$ electronic state of the OH molecule. In the presence of the collision partners He, Ar, H_2, D_2 and N_2 (represented below by M), we have measured the rates for

$$OH\ (A^2\Sigma^+,\ v_i,N_i,J_i) + M \rightarrow OH\ (A^2\Sigma^+,\ v_f,N_f,J_f) + M,$$

where v, N and J refer to quantum numbers for vibration, rotation, and total angular momentum, respectively. While neither the states of the collision partners, nor the individual translational states and angle variables, are resolved, some important trends concerning the dependence of the rate on the OH quantum states have been discovered.[2]

[1] See, e.g., "State-to-State Chemistry," ACS Symposium Series 56 (1977).

[2] R. K. Lengel and D. R. Crosley, "Rotational Dependence of Vibrational Relaxation in $A^2\Sigma^+$ OH," Chem. Phys. Lett. 32, 261-264 (1975).

This article forms the second of a series of three which chronicle these measurements. The first,[3] referred to below as I, describes rotational energy transfer within the v=0 level of $A^2\Sigma^+$ OH. It also contains many of the experimental details common to those measurements and the ones reported here. The third,[4] referred to as III, deals with an information theoretic[5] analysis of the results of I and the present study. An explication of all three parts is contained in the thesis[6] of one of the authors (RKL), which forms the basis for this series.

We here describe our experiments on (exoergic) vibrational energy transfer within the A-state of OH (and the isotopic analog OD). The transfer processes studied are $v_i \rightarrow v_f = 1 \rightarrow 0$, $2 \rightarrow 1$ and $2 \rightarrow 0$, referred to below by this numerical designation (e.g., the cross section $\sigma_{2\text{-}1}$). Individual initial states N_i, J_i are prepared by selective excitation with a frequency doubled, tunable laser. Final state distributions over N_f, J_f are measured by means of rotationally resolved fluorescence. This is illustrated schematically for the 1-0 transfer in Fig. 1 (in which the rotational levels are not shown). The laser provides excitation in the (1,0) band of the A-X system. In the presence of a known pressure of fill gas, collisional transfer to v=0 occurs (as well as rotational transfer within v=1, and overall quenching of the $A^2\Sigma^+$ state, neither of

[3] R. K. Lengel and D. R. Crosley, "Energy Transfer in $A^2\Sigma^+$ OH. I. Rotational," J. Chem. Phys. 67, 2085-2101 (1977).

[4] R. K. Lengel and D. R. Crosley, "Energy Transfer in $A^2\Sigma^+$ OH. III. Surprisal Analysis," to be published.

[5] R. D. Levine and R. B. Bernstein, "Energy Disposal and Energy Consumption in Elementary Chemical Reactions; The Information Theoretic Approach," Acct. Chem. Res. 7, 393-400 (1974).

[6] R. K. Lengel, "Energy Transfer in $A^2\Sigma^+$ OH," Ph.D. Thesis, University of Wisconsin, Madison, WI, June 1976.

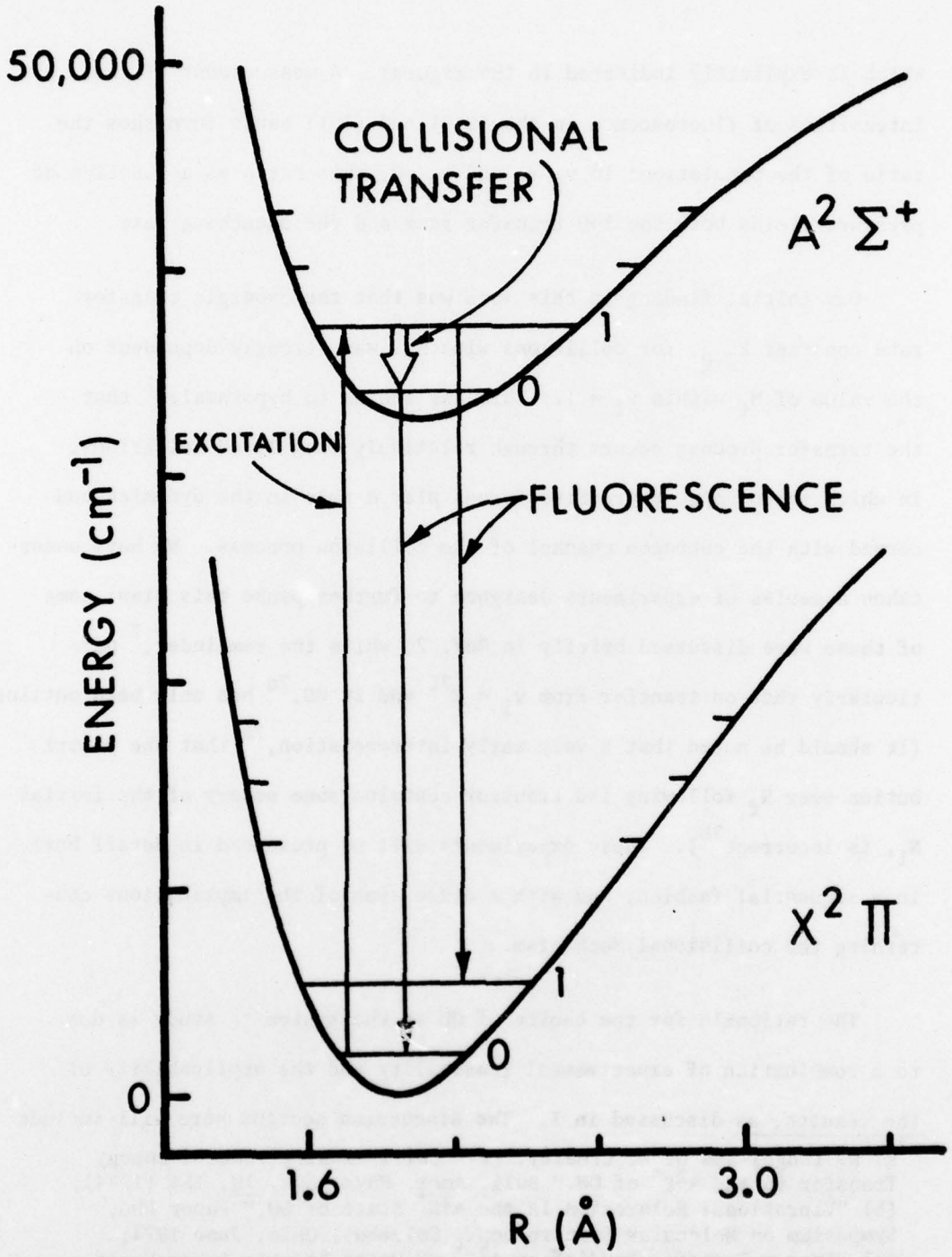

Figure 1. The basic concept of the experiment, illustrated for $1 \rightarrow 0$ transfer. $v_i = 1$ is populated through absorption in the (1,0) band; collisions cause some OH molecules to be transferred to the $v_f = 0$ level. The populations are monitored by observations in the (0,0) and (1,1) bands. Not shown on the diagram are individual rotational levels, nor are indicated the simultaneously occurring processes of rotational energy transfer and overall quenching of the A-state.

which is explicitly indicated in the figure). A measurement of the intensities of fluorescence in the (0,0) and (1,1) bands furnishes the ratio of the populations in v_i =1 and v_f =0; this ratio as a function of pressure yields both the 1→0 transfer rate and the quenching rate.

Our initial finding in this work was that the exoergic transfer rate constant k_{1-0}, for collisions with H_2, was strongly dependent on the value of N_i within v_i = 1. This has led us to hypothesize[2] that the transfer process occurs through relatively long lived collisions, in which anisotropic attractive forces play a role in the dynamics concerned with the entrance channel of the collision process. We have undertaken a series of experiments designed to further probe this view; some of these were discussed briefly in Ref. 2, while the remainder,[7] particularly that on transfer from v_i = 2[7c] and in OD,[7e] has only been outlined. (It should be noted that a very early interpretation,[7a] that the distribution over N_f following 1→0 transfer contains some memory of the initial N_i, is incorrect[7b]). These experiments will be presented in detail here, in a sequential fashion, and with a discussion of the implications concerning the collisional mechanism.

The rationale for the choice of OH as the system to study is due to a combination of experimental feasibility and the applicability of the results, as discussed in I. The discussion section here will include

[7] R. K. Lengel and D. R. Crosley, (a) "Collisionally Induced Energy Transfer in the $A^2\Sigma^+$ of OH," Bull. Amer. Phys. Soc. 19, 154 (1974); (b) "Vibrational Relaxation in the $A^2\Sigma^+$ State of OH," Paper FD6, Symposium on Molecular Spectroscopy, Columbus, Ohio, June 1974; (c) "Energy Transfer Studies on $A^2\Sigma^+$ OH Using Tunable Laser Excitation," Paper TH6, Symposium on Molecular Spectroscopy, Columbus, Ohio, June 1975; (d) "Energy Transfer in $A^2\Sigma^+$ OH," Paper TC1, Symposium on Molecular Spectroscopy, Columbus, Ohio, June 1976; (e) "State-to-State Relaxation in $A^2\Sigma^+$ OH and OD," in Ref. 1.

comment on some uses of the energy transfer rates. We will also make some comparison of our results with recent studies carried out by other investigators. It should be noted that a comprehensive compilation of kinetic data on $A^2\Sigma^+$ OH and OD, through mid-1976 literature and with comment, is contained in the review by Schofield.[8]

EXPERIMENTAL DETAILS

The experimental apparatus and technique used to study the vibrational energy transfer is the same, with minor modifications, as that described in I for the investigation of rotational transfer. Briefly, OH is produced in a fast flow system by the reaction of H atoms* with NO_2. The OH is excited, in the presence of a known amount of fill gas, to a particular v', N', J' level** with the frequency doubled tunable dye laser, and the resulting fluorescence is dispersed and detected with a small scanning monochromator and associated electronics. The modifications here consisted of changes in the spectral regions of excitation and observation, and in the method of presentation of the final spectra.

Molecules were excited to the v'=1 level by absorption in the (1,0) band, and to the v'=2 level via the (2,1) band; all observations were made in the $\Delta v=0$ bands. The (1,0) band was used because of the low population

[8] K. Schofield, "Critically Evaluated Chemical Kinetic Rate Constants for Gaseous Reactions of Electronically Excited Species," J. Phys. Chem. Ref. Data, in press.

* D_2O was substituted for H_2O as the atom source in the OD experiments.

** Standard spectroscopic notation is sued, where single and double primes denote levels of the electronically excited and the ground state, respectively. Hence v_i and v_f are always single primed quantities.

found in this experiment for v''=1, and the (2,1) band was used because of the lack of laser output in the (2,0) absorption region. The use of different bands for excitation and observation reduced the problem of detecting scattered laser light, thus allowing the use of a three-pass excitation scheme as well as a more efficient mode of collection of the fluorescence for use in the normalizing channel of the boxcar averager. It was determined experimentally (see below) that vibrational transfer in OH is independent of the electron spin component, i.e., $\sigma_{1\text{-}0}(J_i = N_i + \frac{1}{2}) = \sigma_{1\text{-}0}(J_i = N_i - \frac{1}{2})$ for the same N_i, within experimental error. Therefore, Q_1 excitations[9] were generally employed here, even though the Q_1' line was usually also overlapped by the laser, thus populating (unequally) both spin components of the same given N_i. (Due to their greater line strength, Q_1 lines are advantageous over the P_1 lines used in I - where it was important to excite only the F_1 component having $J = N + \frac{1}{2}$). In certain cases physics (*viz.* there is no level with N''=0) or instrumental limitations (the laser bandwidth as compared to OH line separations) required the use of other lines to populate a desired level.

The excitations in the (2,1) band produced very weak fluorescence, necessitating the use of much wider spectrometer slits to provide an acceptable signal-to-noise ratio. The simultaneous normalization used in the other experiments had to be abandoned for these excitations, and background subtraction was needed to reduce the effects of the light

[9]The rotational branch terminology is that normally employed for OH; see G. H. Dieke and H. M. Crosswhite, "The Ultraviolet Bands of OH," Johns Hopkins University Bumblebee Report No. 87 (1948), republished in J. Quant. Spectrosc. Radiat. Transfer 2, 97-199 (1962).

scattered from the discharge used for H atom production. This was accomplished by delaying the gate of one channel of the boxcar until after the fluorescence had decayed, and displaying the difference of the two channels.

The intensity of each band was electronically integrated as well as displayed in its rotationally resolved form (see Fig. 2 of I). This integrated intensity $I_{v'v''}$ is proportional to the population $N_{v'}$ of the emitting level

$$I_{v'v''} = c\, A_{v'v''}\, R(\nu)\, \nu^3 N_{v'} \qquad (1)$$

where $A_{v'v''}$ is the appropriate Einstein coefficient for emission, ν the center frequency of the band,* and $R(\nu)$ represents the response of the spectrometer and detector. Eq. (1) is valid if the linewidths are determined by the spectrometer which is the case here. The $I_{v'v''}$ are thus obtained from an integral of the line spectrum vs. wavelength; experimentally this is accomplished using electronic analog integration (vs. time) of the output of the boxcar while the monochromator was scanning (schematically shown in Fig. 2 of I). The linearity and stability of this integration scheme were checked by its ability to produce: (i) a constant slope output with a constant voltage input; (ii) a level output with no input; and (iii) area ratios which were in agreement with those obtained by several manual determinations of the areas of concurrently recorded line spectra, using a calibrated planimeter. Although overlapping

*Inclusion of ν on a line-by-line basis forms a negligible correction.

of vibrational bands can cause problems with such area determinations, it was not a problem here for the v'=1 excitations. Our determination of the rotational distribution of molecules transferred to v_f=0 in the 1→0 transfer process indicates that less than 1% of the intensity of the (0,0) band occurs beyond the nominal band cutoff of 3123.9Å, which we use as the separation point between (0,0) and (1,1). Though overlapping is present in the studies where v_i=2, it is accounted for in the data analysis (see below).

Unlike the rotational transfer experiments where the emission intensities are simply related to relative populations by accurate theoretical line strengths, the area ratios determined experimentally must be corrected for $R(\nu)$ and converted to relative populations using the $A_{v'v''}$, per Eq. (1). The measurement of the spectrometer response and the determination of reliable ratios of the necessary Einstein coefficients are described in detail in reference 10 for OH, and reference 11 for OD.

DATA AND ANALYSIS

The essential results of the experiment are shown in the three exemplary line spectra displayed in Fig. 2. (It is the electronically integrated form of these which is the input to Eq. (1).) In each case the laser is tuned to the $Q_1 3$ line of the (1,0) band, exciting v_i=1,

[10] D. R. Crosley and R. K. Lengel, "Relative Transition Probabilities and the Electronic Transition Moment in the A-X System of OH," J. Quant. Spectrosc. Radiat. Transfer 15, 579-591 (1975).

[11] D. R. Crosley and R. K. Lengel," Relative Transition Probabilities in the A-X System of OD," J. Quant. Spectrosc. Radiat. Transfer 17, 59-71 (1977).

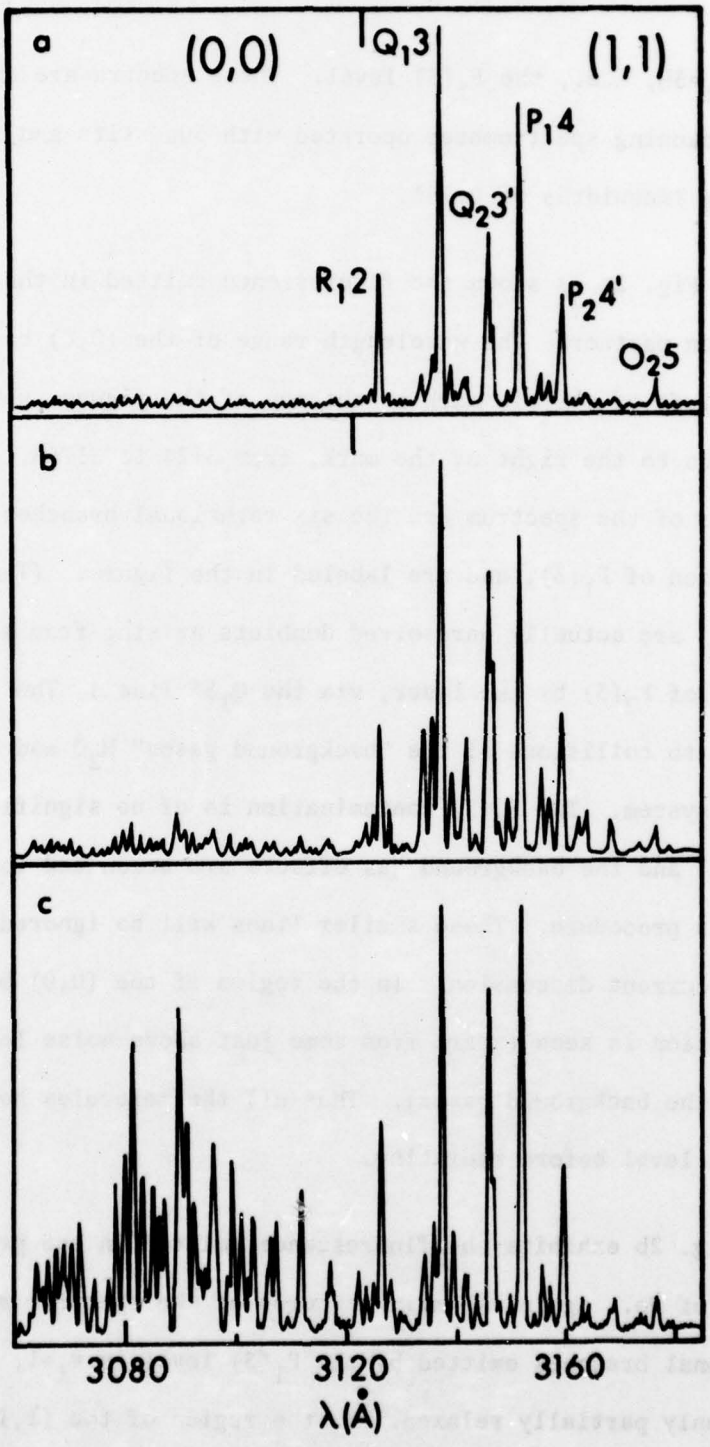

Figure 2. Exemplary experimental data. In each case the $F_1(3)$ level is pumped in $v_i = 1$; the six rotational branches emitted by this level are marked in (a). The (0,0) band lies to the left of 3120Å and the (1,1) band is to the right of that wavelength. (a). Emission in the presence of no added gas. (b) Emission in the presence of about 1 torr of He. (c) Emission in the presence of about 1 torr of H_2.

N_i=3, J_i=3½, i.e., the $F_1(3)$ level. These spectra are obtained with the 0.35m scanning spectrometer operated with 50μ slits and in second order, yielding linewidths of 0.75Å.

In Fig. 2a is shown the fluorescence emitted in the absence of any collision partner. The wavelength range of the (0,0) band is 3064-3124Å, to the left of the tic mark at the top of the figure, while the (1,1) band lies to the right of the mark, from 3124 to 3176Å. The predominant features of the spectrum are the six rotational branches expected from excitation of $F_1(3)$, and are labeled in the figure. (The $R_1 2$, $Q_1 3$, $Q_2 3'$ and $P_2 4'$ are actually unresolved doublets arising from some concurrent pumping of $F_2(3)$ by the laser, via the $Q_1 3'$ line.) The smaller lines are due to collisions of the "background gases" H_2O and NO_2 always present in the system. The $F_2(3)$ contamination is of no significance, as will be seen, and the background gas effects are accounted for in the data analysis procedure. These smaller lines will be ignored for the purposes of the current discussion. In the region of the (0,0) band practically no emission is seen (apart from some just above noise level and also due to the background gases). Thus all the molecules here remain in the initial level before radiating.

Fig. 2b exhibits the fluorescence emitted in the presence of about 1 torr of He. Again the main features of the spectrum are the same six rotational branches emitted by the $F_1(3)$ level in v_i=1, showing that the OH is only partially relaxed. In the region of the (1,1) band now, though, significant emission from other rotational branches can be seen, such as the $Q_1 1$(3135 Å), $Q_1 2$(3136 Å), $Q_1 4$(3140 Å), and the $P_1 2$(3143 Å)

lines that surround the $Q_1 3$ line. The clearly discernable features in the (0,0) band, particularly the Q_1 lines at 3080Å and the Q_2 head at 3090Å, show that some vibrational energy transfer has also taken place. The amount of vibrational transfer which has occurred at this pressure is clearly less than the amount of rotational transfer within $v_i=1$. (In actuality, since the ratio[10] $A_{00}/A_{11} = 1.71$, the results of Fig. 2 indicate an apparent population ratio N_0/N_1 larger than the true value.) This means that the rotational transfer rate is greater than the vibrational transfer rate, for He collisions. This is in clear accord with the expectations concerning energy transfer processes, since the energy level differences for rotational transfer are much smaller ($E(N=3) - E(N=2) \sim 100$ cm^{-1}) than that for the vibrational transfer (~ 3000 cm^{-1}).

Fig. 2c illustrates the profoundly different situation existing for a diatomic collision partner. Here the fill gas is H_2, also at about 1 torr. Considering first the (1,1) band, the same six lines are again evident. There is also clearly shown the presence of some rotational transfer within $v_i=1$, although less than in Fig. 2b for He. The (0,0) band, on the other hand, is very intense, showing that a large amount of vibrational transfer is occurring here. In fact, the total number of molecules in $v_f=0$ is significantly larger than the number in rotational levels other than the initially excited one within $v_i=1$. This is contrary to the expectations concerning relative rates of vibrational and rotational transfer.

The fact that little rotational transfer has occurred within $v_i=1$ means that most of the vibrationally transferred molecules have come from the initially pumped level $F_1(3)$. We may thus identify the

rate measured by these intensity ratios as specific to the level N_i=3; by tuning the laser to different absorption lines, $\sigma_{10}(N_i)$ can be determined.

The Steady State Equations, and Some Corrections Thereto

The data are analyzed by means of a steady-state approximation applied to the level(s) into which the energy transfer occurs. For the case of 1→0 transfer, we write

$$\frac{dN_0}{dt} = N_1 V_{10} P - N_0(1 + Q_0 P) = 0 \qquad (2)$$

where P is the pressure (Torr) of collision partner, V_{10} is the transfer rate, and Q_0 is the rate for quenching v_f=0 of the $A^2\Sigma^+$ state. The radiative decay of v_f = 0 is assigned a rate constant of 1; that is, we measure rates in units of the radiative lifetime τ_0. Thus the working units of our measured rates will be per Torr per lifetime, which presume no absolute parameters such as τ_0 or the temperature. Eq. (2) is considerably simpler than the equations used to analyze the rotational transfer data (see I), since here we have only a two-level system in which the 0→1 back-transfer can be totally ignored.

Some corrections must be applied to Eq. (2) to render it fully appropriate for our experiment. The first of these (see I) follows from a recognition that the population N_0 is not really under steady-state conditions; rather, the laser provides exciting radiation into v_i=1 as a pulse with width ≈ $\tau_0/8$, and the total A-state population (N_1 + N_0)

decays in time with a rate* $(1 + Q_0P)$. Our use of a pulse-stretching preamplifier, integrating the signal over almost all time $(33\tau_0)$, renders the use of Eq. (2) nearly correct, as is discussed in Appendix A of I. The correction to Eq. (2) due to the finite laser pulse width is negligible, and that due to the finite integration period requires the use of an effective radiative lifetime of $1.03\tau_0$. These corrections are explicitly derived in Appendix A of this paper.

Fig. 2a demonstrates that the effect of collisions with the background gases cannot be ignored. These cause both vibrational transfer and quenching at the rates V_b and Q_b respectively (they are always maintained at the same pressure), so that Eq. (2) should read

$$\frac{dN_0}{dt} = N_1(V_{10}P + V_b) - N_0(1 + Q_0P + Q_b) = 0.$$

The rate V_b is measured from runs with no added gas (see Fig. 2a) to be 0.076 ± 0.006 Torr^{-1} τ^{-1}. The determination of Q_b is described in Appendix B; for working purposes it is treated as another adjustment (a 26% decrease) in the radiative lifetime. While these effects of the background gases are always accounted for in the actual analysis, and show up in the data plotted in Figs. 3 and 6, they will be ignored in all the ensuing discussion.

Analogous equations for the populations of the $v_f = 1$ and 0 levels are written for the experiments in which $v_i = 2$:

*Given that Q_1 is not much greater than Q_o; see below.

$$\frac{dN_1}{dt} = N_2 V_{21} P - N_1(\tau_0/\tau_1 + \bar{V}_{10} P + Q_1 P) = 0 \qquad (3a)$$

$$\frac{dN_2}{dt} = N_2 V_{20} P + N_1 \bar{V}_{10} P - N_0(1 + Q_0 P) = 0 \qquad (3b)$$

where τ_1 and Q_1 are analogous to τ_0 and Q_0. $\bar{V}_{10}$ represents an average of $V_{10}(N_i)$ over the rotational distribution produced within $v_f = 1$ by the 2→1 transfer. The assumptions necessary to convert (3a) and (3b) to usable working equations, and the determination of a pertinent value for $\bar{V}_{10}$, are discussed in the Results section.

Other Considerations

Scattered light from the laser is not a problem in these experiments, since the excitation and observation bands are different. However, we must consider the possibility of stimulated emission in the excitation line while the laser is on, which could cause effective branching ratios different from those[10,11] appropriate to spontaneous emission. In Appendix C it is shown that this has negligible influence on the population measurements.

When the population of rotational levels is determined by the intensities of individual rotational branches, as in I and in the determination of the N_f distribution here, the effects of the polarization of the laser and directions of propagation of the exciting and fluorescent light must be considered. This is because rotational line strengths calculated for isotropic conditions do not apply to the anisotropic

nature of most laser-induced fluorescence experiments. Most of the intensity data here are taken by integrating the spectrum and thus summing over all rotational branches emitted by a given level. The net anisotropies in such sums are of the order of a few percent[12] instead of the possible factors of two encountered in I. Even so, we carry out the measurements in a 5G magnetic field, sufficient to magnetically depolarize the fluorescence, as is discussed in I.

Our measured rate constants are reported in units of per lifetime per Torr, as noted above. These need no additional parameters to be used directly in, e.g., modelling studies, or the assessment of fluorescence efficiencies, under similar (300°K) temperature conditions. Conversion to rate constants (cm^3 sec^{-1} units) and cross sections (cm^2) requires the absolute value of τ_0 and a choice of translational temperature. We use 0.7 μsec and 320°K respectively. The rationale for these choices is discussed in I.

RESULTS

1 → 0 Transfer Rates

The results for the 1→0 transfer data are obtained by fitting the population ratio N_0/N_1, obtained from I_{00}/I_{11}, to the rearranged form of Eq. (2),

$$N_0/N_1 = V_{10}P/(1 + Q_0P), \qquad (4)$$

[12] D. R. Crosley, "Level Crossings and Anisotropic Emission in a $^2\Sigma$ - $^2\Pi$ Transition," BRL Report (to be published).

by means of a non-linear least-squares regression package. Plots for H_2 and He (in the form I_{00}/I_{11}) are shown in Fig. 3.

In the case of H_2, three different values of N_i (0,3 and 5) are pumped. As is evident from the plot, there is a definite dependence of the intensity ratio vs. pressure curves upon the rotational level of the OH which is undergoing the transfer. The vertical bars in Fig. 3 show the <u>total spread</u> in the ratios obtained from multiple determinations, a minimum of four, at each pressure. (This does not include occasional "bad" runs, which are classified as such not because of a nonconformity to the average but, rather, *a priori* on the basis of severe drift of laser power, cell pressure, etc.). The curvature in the plots, tending to an asymptotic freezing-in of (an N_i- dependent) N_1/N_0 ratio at high pressure, is due to the quenching from $v_f = 0$. All of the H_2 data points for these three N_i values are fit together to the four parameters $V_{10}(0)$, $V_{10}(3)$, $V_{10}(5)$ and Q_0. One quenching rate constant is appropriate for <u>all</u> the data since it is the quenching of $v_f = 0$ which enters into Eq. (2). (This would be invalid if Q_0 depended strongly on N_f, <u>and</u> the distribution over N_f varied with N_i. But neither is the case. German's results[13] show Q_0 essentially independent of N in v' = 0, and the N_f distributions are seen below to be nearly identical). The numerical results are given in Table 1.

With He as a collision partner, the rate V_{10} is clearly much smaller, as is already evident from Fig. 2. The intensity ratio determinations

[13] K. R. German, "Collision and Quenching Cross Sections in the $A^2\Sigma^+$ State of OH and OD," J. Chem. Phys. <u>64</u>, 4065-4068 (1976).

TABLE 1. RESULTS FOR 1 → 0 TRANSFER IN OH. ERROR BARS ARE THOSE FROM LINEFIT CONFIDENCE LIMITS ONLY.

COLLISION PARTNER	QUANTITY	N_i	RATE $torr^{-1}\tau^{-1}$	RATE CONSTANT $10^{-10}cm^3sec^{-1}$	CROSS SECTION $Å^2$
H_2	V_{10}	0	4.0±0.2	1.89±0.09	9.7±0.6
		3	3.3±0.2	1.56±0.09	8.1±0.5
		5	2.5±0.2	1.18±0.09	6.1±0.4
	Q_0	-	1.9±0.2	0.90±0.09	4.6±0.5
D_2	V_{10}	0	4.9±0.3	2.32±0.14	15.9±1.1
		3	3.7±0.3	1.75±0.14	12.3±0.9
		5	2.8±0.2	1.32±0.14	9.3±0.7
	Q_0	-	2.3±0.3	1.09±0.09	7.4±0.9
N_2	V_{10}	0	4.2±0.2	1.99±0.09	24.7±1.3
		3	3.5±0.2	1.66±0.09	20.8±0.9
		5	2.1±0.1	0.99±0.05	12.6±0.6
	Q_0	-	0.98±0.11	0.46±0.05	5.8±0.7
He	Q_0	-	0.028±0.008	0.013±0.004	0.09±0.03
Ar	Q_0	-	0.067±0.008	0.032±0.004	0.42±0.05

(several at each pressure) are shown in Fig. 3; on an expanded scale a definite linear increase with pressure is clear. For both He and Ar (which appears quite similar to He), the scatter in the data is relatively large. This makes it impossible to discern any curvature in the plots, at or below our highest available working pressure of 1.5 torr, and a quenching rate cannot be extracted. The quenching rates are therefore set equal to zero and linear least squares fits of the data are used to obtain the transfer rate constants, which are given in Table 1. The previously reported[14] values of Q_0 for Ar and He are ~ 10% of these V_{10} and are thus compatible with the data shown; that is, they are not large enough to produce a measureable curvature. There is also no possibility of determining from this data any dependence of the V_{10} upon N_i, since the scatter masks any differences that might be present in the plots, which contain points for excitations to N_i = 0 and 3 for He. Even with less scatter, any dependence upon the initial rotational level would be difficult to discern because rotational transfer within the v_i = 1 level is rapid enough compared to vibrational transfer to wash out any rotational dependence.

The clear difference between the monatomic gases and H_2 indicates to us that the internal degrees of freedom of the diatomic play some role (probably compounded by the ability to form a longer-lived, 4-center collision entity, as discussed below). Now this could show up simply as an increase in V_{10} with the number of open energy channels for the products, or through some resonant, near-zero energy defect match between OH and its partner.

[14] P. Hogan and D. D. Davis, "Comments on 'Electronic Quenching and Vibrational Relaxation of the OH ($A^2\Sigma^+$, v'=1) State'," J. Chem. Phys. 64, 3901 (1976).

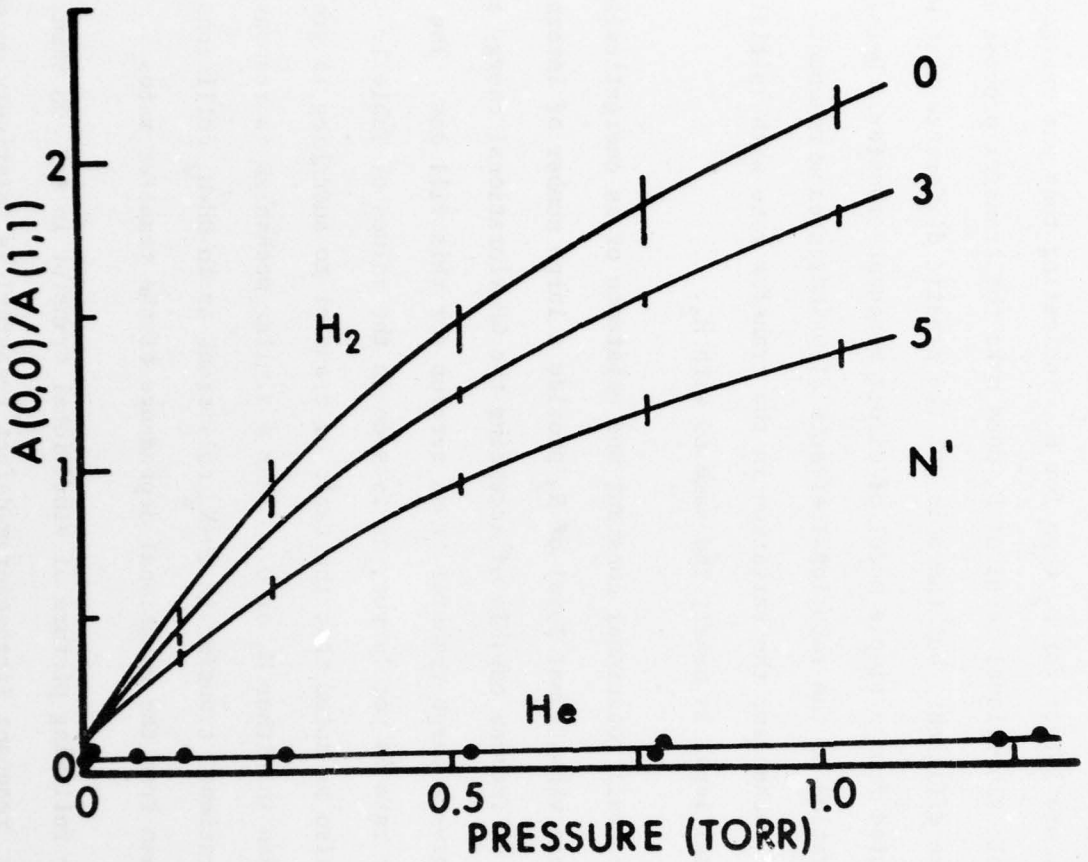

Figure 3. Plots of the ratio of the integrated intensity of the (0,0 band to that of the (1,1) band, as a function of pressure of H_2 and He. For H_2, data for three different initial rotational levels are shown; the data for He includes several values of N_i'. For H_2, the vertical lines represent the total spread in all the data at that pressure; the curves are the results of the non-linear least squares fit to the four parameters which describe the data. The non-zero intercepts at zero pressure are caused by collisions with the background gases, and are accounted for.

D_2 furnishes a test of the latter, since its vibrational energy spacing is within 4 cm^{-1} of that of $A^2\Sigma^+$ OH. That transfer in D_2 is not much more efficient than in H_2 can be seen from the rates in Table 1. They are larger for D_2 than for H_2, indicating that the energetically accessible vibrational level of D_2 does make the transfer process somewhat more efficient, but there is not the drastic difference that would be expected from a simple model of direct resonant transfer. Detailed consideration of the rotational effects also indicates no resonant transfer mechanism; the variation in the transfer rate with initial rotational level is nearly the same as with H_2.

The small rotational constant and existence of an energetically accessible vibrational level of N_2 provide a large number of internal degrees of freedom capable of accepting the OH vibrational energy and should give a large transfer cross section for this fill gas. The transfer rate is yet larger, as is seen in the values of Table 1. It should also be noted that the ratio of transfer to quenching is greater in N_2 than in either H_2 or D_2. That a similar mechanism is responsible for vibrational transfer in OH-N_2 collisions as in OH-H_2 collisions is again seen from the rotational dependence of the transfer rates.

The following picture of vibrational transfer in $A^2\Sigma^+$ OH then emerges: resonant (zero-energy-defect transfer) is relatively unimportant, but diatomic collision partners, with their internal degrees of freedom, have cross sections one to two orders of magnitude larger than the rare gases, and the transfer rate, at least for the diatomic collision partners, is a strong function of the initial rotational level of the OH.

Rotational Dependence of V_{10}

The dependence of V_{10} on N_i, as seen from Fig. 3 and Table 1, is quite large. We have hypothesized[2] that it is due to effects on the entrance channel collision dynamics in the following way. The early part of the collision between OH and its diatomic collision partners is governed by anisotropic attractive forces (dipole-induced dipole). A favorable orientation will lead to a long-lived collision which is quite efficient in transferring energy from the OH vibration to the internal degrees of freedom of the collision partner, as well as to OH rotation (see below). The non-rotating OH molecule provides an opportunity for easier establishment of this sticky collision, but a rotating OH molecule tends to wash out the anisotropy and presents a less favorable entrance channel. A similar effect has been proposed[15] concerning trajectory studies of HF-HF vibrational relaxation as a function of J, and has received indirect experimental support in that such a mechanism can explain the minimum observed in the temperature dependence of the thermally averaged rate for that energy transfer process.[16] The OH - H_2, D_2 or N_2 collision pairs do not possess the strong dipole-dipole forces of HF-HF encounters, but indications of the same effect (albeit smaller) can be found in the thermally averaged vibrational relaxation of DF by H_2.[17]

---

[15] G. C. Berend and R. L. Thommarson, "Vibrational Relaxation of HF and DF," J. Chem. Phys. 58, 3203-3208 (1973).

[16] J. F. Bott, "HF Vibrational Relaxation Measurements Using the Combined Shock-tube-laser-induced Fluorescence Technique," J. Chem. Phys. 57, 96-102 (1972).

[17] J. F. Bott, "Vibrational Relaxation of HF(v-1) and DF(v-1) by H_2 and D_2," J. Chem. Phys. 61, 2530-2535 (1974).

It is thus desirable to measure the N_i dependence of V_{10} for higher values of N_i. Due to decreasing populations with increasing J in the X-state, the signal-to-noise ratio rapidly deteriorates for higher N_i and a full study of the pressure dependence of N_0/N_1 is precluded. Rather the data were taken in the following way. At a single pressure of fill gas (0.56 torr for H_2, 0.57 torr for N_2), the ratio N_1/N_0 was determined as a function of N_i. Using the value of Q_0 obtained by fitting the full set of data for N_i = 0, 3 and 5, Eq. (4) was used to determine relative values of $V_{10}(N_i)$. These were then normalized to the N_i = 0,3,5 values. The results, in the form of cross sections σ_{10}, are listed in Table 2 and plotted in Fig. 4.

A continuing and smooth fall-off of σ_{10} with N_i (at least up to N_i = 7 or 8) can be seen, in accord with the picture of increasing rotation washing out the anisotropic attractive forces. It is important to note that the known variation of A_{11} with N is in the wrong direction[10,11] to account for these differences.

The leveling off at high values of N_i could at first glance be ascribed to rotational transfer occurring into lower rotational levels of v_i = 1 followed by vibrational transfer into v_f = 0. That is, the cross section of about 4Å^2 would then represent the rotational transfer cross section out of these high-N levels. This is not the case, as is evidenced in the rotationally resolved scans of the (1,1) band, which exhibit a reasonably clean single level spectrum like those in Fig. 2. Further, a model of the rotational relaxation's competition with vibrational relaxation shows that these σ_{10} can be attributed to the single

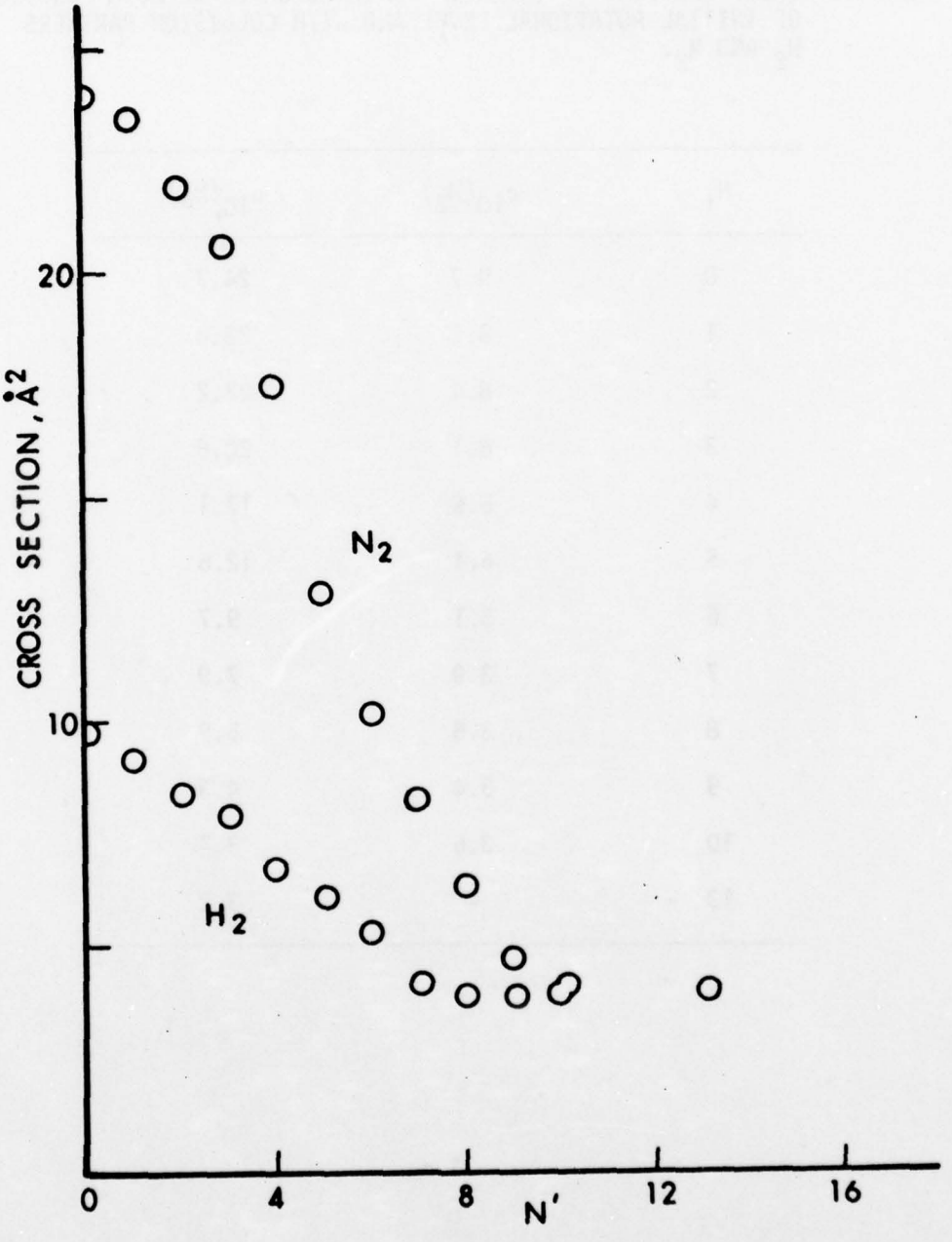

Figure 4. Cross sections for $1 \rightarrow 0$ transfer as a function of initial rotational level in $v_i = 1$, for H_2 and N_2. The point at $N_i = 13$ is an N_2 cross section.

TABLE 2. CROSS SECTIONS ($Å^2$) FOR $1 \rightarrow 0$ TRANSFER IN OH AS A FUNCTION OF INITIAL ROTATIONAL LEVEL AND WITH COLLISION PARTNERS H_2 AND N_2.

N_i	$\sigma_{10}(H_2)$	$\sigma_{10}(N_2)$
0	9.7	24.7
1	9.2	23.0
2	8.4	22.2
3	8.1	20.8
4	6.6	17.1
5	6.1	12.6
6	5.1	9.7
7	3.9	7.9
8	3.6	5.9
9	3.4	4.3
10	3.6	3.7
13	-	3.2

level alone; this 'rotational averaging' analysis is carried out in III using the rotational rates of I and surprisal analysis to estimate rates for high values of N. Thus, the bell shapes of the curves are suggestive of a different mechanism responsible for the transfer from high values of N_i, where the anisotropy may be fully averaged by rapid rotation. A simple energy defect dependence of the transfer rate is inadequate to explain the N_i dependence of V_{10}. As will be discussed below, the transferred molecules have a nascent rotational distribution such that the OH loses an average net energy of 2650, 2850, and 3140 cm^{-1} in transfer from N_i = 0, 3, and 5 respectively; though a quantitative measurement is difficult at higher N_i, the appropriate figure is 3800 cm^{-1} for N_i = 8. We have been unable to fit the results shown in Fig. 4 to these energy defect values, although a surprisal analysis (see III) codifies them neatly and is very suggestive of the separate high-N_i mechanism. The N_i dependence exhibited in Table 1 can be further used to rule out resonant exchange. Fo example, transfer from N_i = 5 into the observed N_f distribution within v_f = 0 would be favored by the near match to the change in D_2 of v_i = 0, J_i = 1 → v_f = 1, J_f = 2. Second most probable would be transfer from N_i = 3, matched to the D_2 transition v_i = 0, J_i = 3 → v_i = 1, J_i = 3. Other examples, all of which run counter to the smooth decrease seen, can be conjectured depending on a choice of ΔJ propensity rules for the collision partner.

If the collision dynamics are responsible for the dependence of V_{10} on N_i, then both F_1 and F_2 levels, with $J = N \pm \frac{1}{2}$ respectively, should yield the same transfer rate. A series of measurements on H_2

and N_2 were made using the $R_2 2$ pump line (yielding pure $F_2(3)$), the $P_1 4$ pump (pure $F_1(3)$), and the $Q_1 3$-$Q_1 3'$ combination ($F_1(3)$ and $F_2(3)$ in about a 5 to 1 ratio). The results for V_{10} are identical to within the experimental error of 6%, so that rotation only, not total angular momentum, is important. We conclude that it is indeed the dynamics of the collision process which govern the dependence found.

Rotational Distribution Within $v_f = 0$

The rotationally resolved spectra (see Fig. 2c) of the (0,0) band have been analyzed as described in I to obtain populations of individual N_f, J_f levels. These measurements were carried out for H_2 as the collision partner, at pressures from 0.1 to 0.4 torr. Over this range there was no discernible dependence of the populations on pressure so the results at the different pressures were averaged. Since the spectra resemble those obtained from sources in thermal equilibrium, it is appropriate to display the populations in a Boltzmann plot, given in Fig. 5. As can be seen from the fitted line, these populations can be well represented by a simple thermal distribution with a temperature of 670±60°K. When the points obtained from excitations to different initial rotational levels of v' = 1 are fit separately, temperatures of 620±20, 670±20 and 680±30°K are found for excitations to N_i = 0, 3, and 5 respectively, so there seems to be some trend toward higher temperatures as initial rotation increases. However, the fitting errors, quoted at the 1σ, prevent drawing any detailed conclusions from the variation. The plot shows only the populations of the F_1 levels in $v_f = 0$; the populations

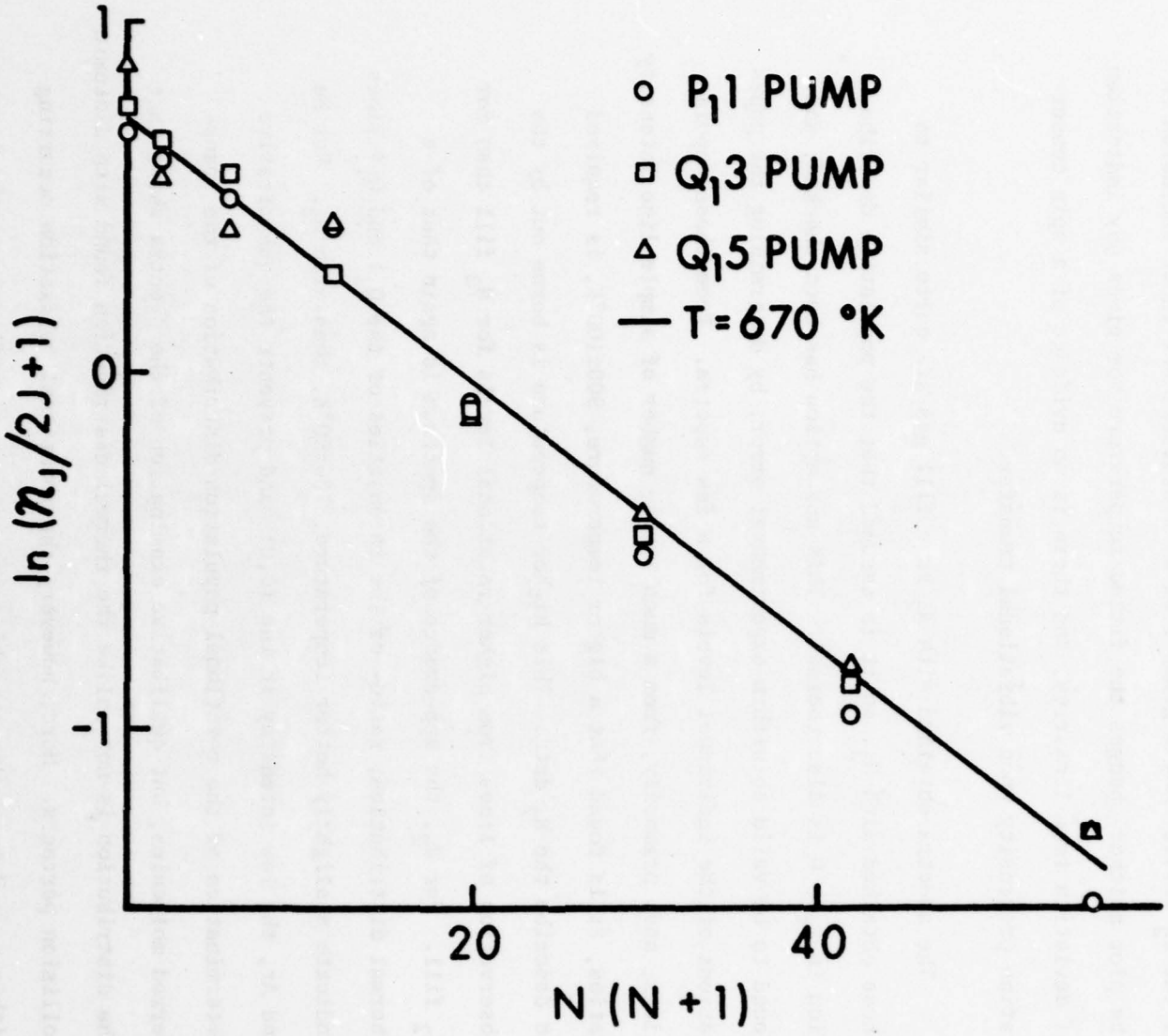

Figure 5. Boltzmann plot of the rotational population distribution in $v_f = 0$ following $1 \rightarrow 0$ transfer, for collisions with H_2. Data for F_1 levels is shown (see text) for three different values of N_i. The line is a least squares fit to a temperature of 670°K.

of the F_2 levels show a great deal more scatter, but their inclusion in the plot neither changes the fitted temperature nor gives any indication of deviation from linearity, and there is no evidence of a spin conservation propensity upon vibrational transfer.

The spectra obtained with N_2 as a fill gas are quite similar to those obtained with H_2, so it is assumed that the population distribution in $v_f = 0$ is also thermal. This assumption has been checked, and found to be valid to within experimental error, by determining the populations of the individual levels for a few spectra. From these populations, and, primarily, from a much larger number of simple line intensity ratios, it is found that a higher temperature, 900±100°K, is required to describe the N_2 data. This higher temperature is borne out by the observation of lines from higher rotational levels for N_2 fill than for H_2 fill. For D_2, the appearance of the spectrum is again that of a thermal distribution; ratios of the intensities of the $Q_1 1$ and $Q_1 4$ lines indicate a slightly hotter temperature, 700±50°K, than with H_2. For He and Ar, the low intensity in the (0,0) band prevents the quantitative determination of the rotational population distribution of the transferred molecules, but qualitative examination of the spectra shows that the distribution is not unlike the thermal distribution found with diatomic collision partners. Here, however, the rotational relaxation occurring within $v_f = 0$ precludes attaching mechanistic significance to the monatomic results.

A question that must be addressed is whether these thermal distributions represent the nascent populations of the transferred molecules or whether they are the result of rotational transfer subsequent to the vibrational transfer. This has been examined for different possible initial distributions. First, a comparison with spectra taken in the rotational transfer experiments (Fig. 3 of I) shows immediately that the population distribution within $v_f = 0$ cannot be due to subsequent rotational relaxation from a single level. Thus the N_f distribution shows no indication of a memory of N_i.

A second possibility is isoenergetic transfer, which leads to selectively populated higher values of N_f. In OH the pair of levels $v_i = 1$, $N_i = 5$ and $v_f = 0$, $N_f = 14$ are 3 cm^{-1} apart; and $v_i = 1$, $N_i = 0$ is separated from $v_f = 0$, $N_f = 13$ by 33 cm^{-1}. ($v_i = 1$, $N_i = 1$ is closer but cannot be as easily investigated in our experiments.) Spectra with H_2 as a collision partner were carefully examined for the $Q_1 13$ and $Q_1 14$ lines of the (0,0) band. A steady state expression for the population of either of these levels, $N(N_f)$ is written as $N(N_f) = V_{10}(N_i,N_f)/(0.9 + QP + RP)$, where R is the total rotational relaxation rate from that level, and the 0.9 reflects a longer radiative lifetime here. R is taken from I as* 8 $torr^{-1}\tau_0^{-1}$. This expression is combined with Eq. (4) to yield the working equation, $V_{10}(N_i,N_f)/V_{10}(N_i, \text{total}) = (0.9 + QP + RP)N(N_f)/(1 + QP)N_0$. The values found are $V_{10}(5,14) = 0.009\ V_{10}(5,\text{total})$ and $V_{10}(0,13) = 0.006\ V_{10}(0,\text{total})$. However, the

*Although Q may increase with N_f, R is probably smaller than this value. The total R+Q = 10 $torr^{-1}\tau_0^{-1}$ is not a critical number here.

N_f distribution expressed as a 670°K temperature yields ratios of 0.003 and 0.007 respectively. Thus an isoenergetic mechanism accounts for well less than 1% of the total vibrational transfer, and the observed distribution is not due to relaxation from high levels. Of course, the smooth variation of $V_{10}(N_i)$, with no maxima at N_i = 1 or 5, is also in disaccord with such a possibility.

Although rotational relaxation subsequent to vibrational transfer is not fast enough to give the measured distributions for the population of either high (isoenergetic mechanism) or low (memory of initial state mechanism) levels, it is possible that the nascent distribution is thermal or near thermal with a temperature higher than that measured. However, there are no systematic deviations, outside of experimental error, found for the temperatures obtained from the steady state experiments at various pressures of H_2 and N_2 below 0.4 Torr. Further, time-domain experiments were carried out in which a high-speed preamp and the variable boxcar gate were used to examine the rotational distribution at fixed pressure but at different times following the excitation pulse. While the time dependence of the total N_0 population was seen to vary as expected, the observed curves were the same for wavelength settings corresponding to different values of N_f.*

In summary here, we conclude that transfer with memory, isoenergetic transfer, or rotational relaxation within $v_f = 0$ is not responsible for the observed thermal distribution. Rather, the nascently transferred

*These measurements were not quantitative, though convincing for the purpose. The spectrometer slits had to be wider, so only low-N, medium-N, and high-N sets were distinguished.

molecules are in the thermal distribution found experimentally. The lack of significant N_i dependence of the distribution for a given collision partner suggests to us that a relatively long-lived, or sticky, collision occurs. (We choose to be deliberately vague about how long-lived we mean; that cannot be addressed directly in these experiments and would be only speculative.) Such a picture also explains the lack of resonant or isoenergetic transfer.

Clearly some of the energy of the initially vibrationally excited OH has been transferred to OH rotation, but most of it (some 80% or more) is transferred into the internal degrees of freedom of the diatomic collision partner (and/or the translational energy of the departing diatomic pairs). This is in line with the overall finding that the diatomic fill gases have larger values of V_{10} than the monatomics; this we have attributed to the participation of the internal degrees of freedom of the former. What is not readily understandable, however, and the only piece of the picture which we feel does not easily fit, is that the amount of energy transferred into OH rotation increases as does the complexity (number of available internal energy level channels) of the collision partner.

Whatever 'collision complex' that may be formed is, however, not sticky enough that the atoms lose their molecular identification. One mechanism by which the transfer for D_2 collisions could take place is a reactive one:

$$OH(v_i = 1) + D_2 \rightarrow OD(v_f = 0) + HD$$

Although both the (0,0) and (1,1) bands of OH and OD are overlapped, the resolution of the monochromator employed is sufficient to provide some areas of the spectra where OD emission lines from either vibrational level would be clearly discernable. No evidence of OD emission is found, which implies, from considerations of the noise in the signals, that the above reaction occurs at a rate of less than three percent of that of the 'direct' transfer. Similarly, no OH could be seen when H_2 was the collision partner in the OD experiments described next. The same reaction for OH + H_2 transfer cannot be directly checked experimentally, but we feel it is ruled out by these deuterated species results.

1 → 0 Transfer in OD

Any mechanism proposed to explain the above results for vibrational transfer in OH should be equally applicable, with only changes to reflect differences in energy levels and mass, to vibrational transfer in the isotopically substituted OD molecule. The only change required in the experiment is the obvious replacement of the H_2O reservoir (for H-atom production) with a sample of D_2O. The pumping lines of the (1,0) band in OD give no possibility of exciting OH, due to the difference in the vibrational spacing of the two molecules. No OH fluorescence is seen in the emitted spectra when OD is excited, and the ground state was found to be reasonably pure OD by experiments deliberately exciting OH.*

*Even though the phosphoric acid rinse of the cell (see I) was with H_3PO_4 not D_3PO_4, and the D_2O used was of undetermined purity.

Experiments were carried out with H_2 and N_2 as collision partners. A plot of the H_2 results, again for the same three N_i levels, is shown in Fig. 6. Results for both gases (τ_0 for OD is also 0.7 μsec[18]) from fits to Eq. (4), are given in Table 3. For mechanism assessment, it is the cross sections which should be compared, not the rates, due to the change in collision velocity with the isotopic change.

The results show that vibrational transfer occurs with nearly the same probability per collision in OH and OD, even though there is quite a difference in the energy defect (970 cm^{-1}) for the two molecules. There appears to be less variation in V_{10} with N_i in OD. However, this can be explained in part by the faster rate of rotational transfer within $v_i = 1$ in OD, which is expected from the results of I and III. This expectation is borne out by qualitative examination of the spectra of the OD, which show more rotational transfer in the (1,1) band than is evident for OH in Figure 2. Such rotational averaging causes a decrease in the observed rates for $N_i = 0$ excitations, little change for $N_i = 3$ excitations, and an increase for $N_i = 5$ excitations as compared with anticipated N_i dependence by analogy to OH.

The smaller rotational spacing of OD also results in a fluorescence spectrum that cannot be as well resolved with the small monochromator employed here, so a detailed examination of the population distribution of the transferred molecules is not possible. It is obvious that the distribution is not decidedly non-thermal, and that the distribution

[18] K. R. German, "Direct Measurement of the Radiative Lifetimes of the $A^2\Sigma^+(v=0)$ States of OH and OD," J. Chem. Phys. 62, 2584-2587 (1975).

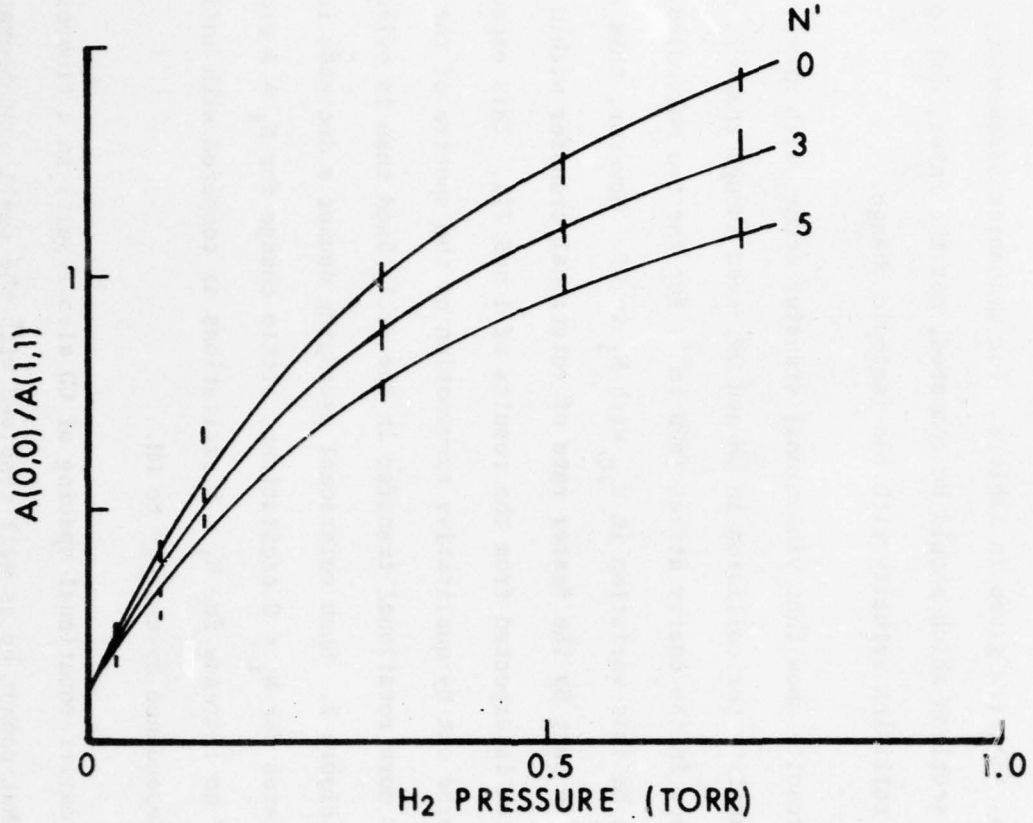

Figure 6. The ratio of the integrated intensities of the (0,0) and (1,1) bands of che OD molecule, for collisions with H_2. Data, curves, and N_i as in Fig. 3.

TABLE 3. RESULTS FOR 1 → 0 TRANSFER IN OD. ERROR BARS ARE THOSE FROM LINEFIT CONFIDENCE LIMITS ONLY.

COLLISION PARTNER	QUANTITY	N_i	RATE $torr^{-1}\tau^{-1}$	RATE CONSTANT $10^{-10} cm^3 sec^{-1}$	CROSS SECTION $Å^2$
H_2	V_{10}	0	3.6±0.3	1.70±0.14	8.7±0.6
		3	3.1±0.2	1.47±0.09	7.6±0.4
		5	2.7±0.2	1.28±0.09	6.6±0.5
	Q_0	-	2.6±0.3	1.23±0.14	6.3±0.8
N_2	V_{10}	0	2.56±0.09	1.21±0.04	15.4±0.5
		3	2.36±0.08	1.12±0.04	14.7±0.5
		5	2.17±0.08	1.03±0.04	13.1±0.5
	Q_0	-	0.73±0.08	0.35±0.04	4.4±0.5

is hotter than room temperature, so there are no gross differences between the N_f distribution in OD and OH.

The lack of occurrence of resonant transfer can also be seen in the results of Table 3, since the vibrational spacing of OD and N_2 is within 100 cm^{-1} of one another, while the vibrational spacing in H_2 is nearly twice as large. We conclude that the mechanistic hypothesis developed for OH is indeed applicable to OD as well.

Transfer From $v_i = 2$

A full picture of vibrational transfer in OH requires knowledge of the dependence of the transfer rate on vibrational as well as rotational level. Our picture of the collision process predicts that $2 \rightarrow 0$ transfer should occur at a comparable rate to that for $2 \rightarrow 1$ or $1 \rightarrow 0$. That is, the fact that nearly twice as much energy is being removed from the OH vibration should be of little concern if the process occurs via a long-lived collision. In addition, we expect to again find that the transfer rates from $v_i = 2$ decrease as N_i increases, since the entrance channel dynamics should not be greatly different.

The weak fluorescence obtained from $v_i = 2$ excitations, especially when spread over the (0,0), (1,1), and (2,2) bands in the transfer experiments, imposes more restrictions than for $v_i = 1$, and several assumptions must be made to reduce measured intensities as a function of pressure into transfer rates. In particular, the data are not of high enough quality to warrant a non-linear fit to Eqs. (3) to obtain

all the parameters involved. We first make the approximation that $Q_1 = Q_0$. This is supported by German's lifetime measurements;[13] those differences in Q_1 and Q_0 which he does find for N_2 (the collision partner studied here) are just at the limit of his error bars and, if real, are too small to affect the present analysis. Although our recommended value[10] of τ_1/τ_0 is 1.09, we set $\tau_1 = \tau_0$ in Eqs. (3). For the range of pressures used, the population in $v_f = 1$ remains small and its loss mechanism is dominated by collisions, not quenching, so that this introduces negligible error (compared with other sources of uncertainty) into the analysis.

Using these two assumptions, Eqs. (3) can first be combined to give an expression for the total rate of transfer out of $v_i = 2$:

$$R_t \equiv (QP + 1)(N_0 + N_1)/N_2 = (V_{21} + V_{20})P \qquad (5)$$

Experimentally, $v_i = 2$, $N_i = 1$ or 4 is excited by absorption of the $Q_1 1$ or $Q_1 4$ line, respectively, in the (2,1) band, and the fluorescence of the (0,0), (1,1), and (2,2) bands is monitored as a function of N_2 pressure. Following a choice of the cutoff wavelength between the (0,0) and (1,1) bands together with some adjustment necessitated by overlapping, as described below, the observed integrated spectral intensities are reduced to populations and fitted to Eq. (5) to obtain the total transfer rate, $V_{21} + V_{20}$. The plot for the two N_i levels is shown in Fig. 7a; Table 4 contains the numerical results. It is immediately clear that the total transfer rate again decreases with N_i, for the two levels probed, and that the total transfer rate at least is of comparable magnitude to V_{10}.

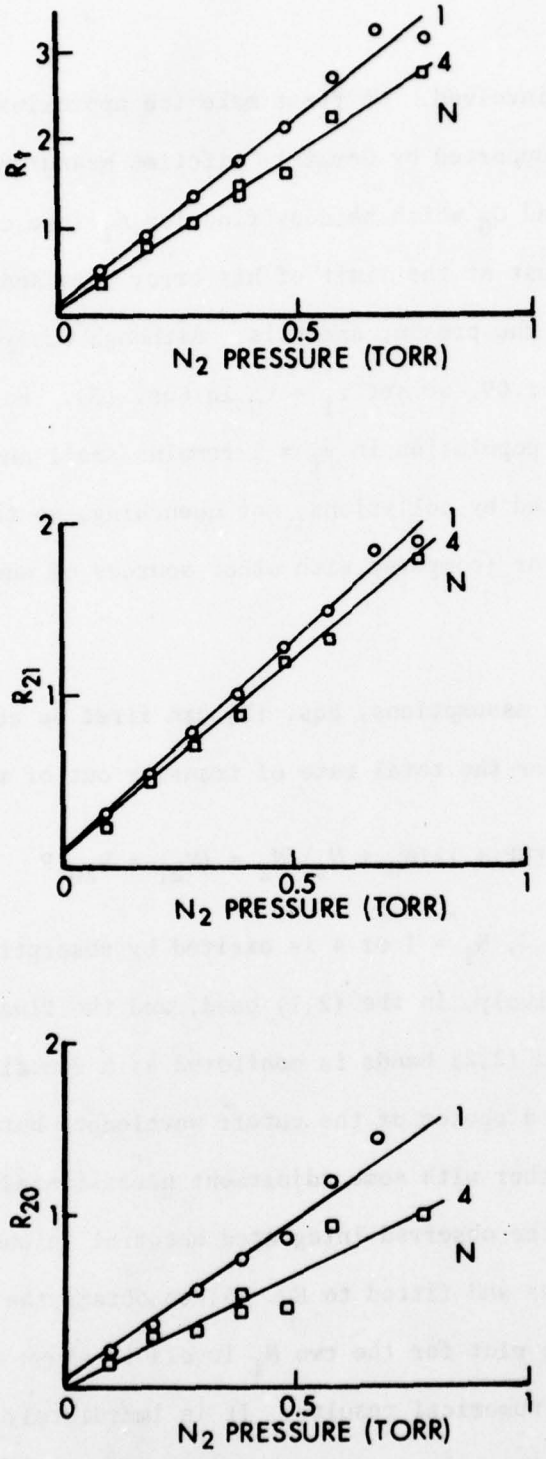

Figure 7. Plots pertinent to transfer from $v_i = 2$ in OH, for collisions with N_2. The circles represent experimental data for $N_i = 1$, and the squares are the data for $N_i = 4$. The straight lines are least squares fits. See text (Equations 5 and 6) for definitions of R_t, R_{21}, and R_{20}. Top: plot pertinent to total transfer out of $v_i = 2$. Middle: plot for single-quantum $2 \rightarrow 1$ transfer. Bottom: plot for two-quantum transfer, $2 \rightarrow 0$.

TABLE 4. RESULTS FOR TRANSFER FROM $v_i = 2$ IN OH, FOR COLLISIONS WITH N_2. ERROR BARS ARE FROM LINEFIT CONFIDENCE LIMITS ONLY.

N_i	QUANTITY	RATE $torr^{-1}\tau^{-1}$	RATE CONSTANT $10^{-10} cm^3 sec^{-1}$	CROSS SECTION $Å^2$
1	$V_{2,total}$	4.3±0.2	2.03±0.09	25.5±1.2
	V_{21}	2.5±0.2	1.18±0.09	14.8±1.2
	V_{20}	1.8±0.2	0.85±0.09	10.7±1.2
4	$V_{2,total}$	3.5±0.1	1.66±0.05	20.7±0.6
	V_{21}	2.3±0.1	1.09±0.09	13.6±1.2
	V_{20}	1.3±0.2	0.61±0.09	7.7±1.2

The analysis to determine the individual transfer rates, V_{20} and V_{21}, is somewhat more complex. Eqs. (3) are rearranged to read:

$$R_{21} \equiv [1 + (\bar{V}_{10} + Q)P]N_1/N_2 = V_{21}P \tag{6a}$$

$$R_{20} \equiv [(1 + QP)N_0 - \bar{V}_{10}PN_1]/N_2 = V_{20}P \tag{6b}$$

Application of these expressions first requires a knowledge of the distribution over rotational levels in $v_f = 1$ following $2 \rightarrow 1$ transfer, so that $\bar{V}_{10}$ can be calculated. The low population in $v_f = 1$ (due to rapid transfer out) yields a low (1,1) band intensity and precludes an experimental measurement of this distribution. By analogy with the $1 \rightarrow 0$ transfer findings, we take it to be thermal, and use the temperature found there. Qualitative examination of the spectra of the (0,1) band reveals no features which would indicate a non-thermal distribution, and the R-head region is not prominent enough (see below) to be consistent with a higher temperature.

Thus we describe the N_f distribution in $v_f = 1$ by a temperature of 900 ± 100°K, yielding $\bar{V}_{10} = 2.48 \pm 0.11$ torr$^{-1}\tau^{-1}$ ($\Delta\bar{V}_{10}$ here reflects ΔT only). The magnitude of the effect of this assumption has been examined. A 15% uncertainty in $\bar{V}_{10}$, which corresponds to a temperature in the range 600 - 1200°K, produces an 8% error in V_{21} and a 10% error in V_{20}, approximately twice the fitting (data scatter) error. Of course, since $\bar{V}_{10}$ is not required for the total transfer rate $V_{21} + V_{20}$, that sum is unaffected by these assumptions. Any gross discrepancies between our calculated $\bar{V}_{10}$ and its true value would then show up as curvature in

the plots of Eqs. (6), and a disagreement between the sum of the separately determined V_{21} and V_{20} compared with the total from the analysis via Eq. (5).

The plots are shown in Figs. 7b and 7c for R_{21} and R_{20} respectively, and numerical results are again collected in Table 4. The good agreement between the sum V_{21} plus V_{20}, and the separately determined total rate, gives us confidence in the analysis procedure used. The results show that V_{20} is of comparable magnitude to V_{21} (and thus to V_{10}).

The rotational distribution in $v_f = 0$ does not enter into the calculations directly, but it is necessary as a source of information about the transfer mechanism and the results are needed to obtain the populations N_1 and N_0 from the intensities of the (0,0) and (1,1) bands. A measure of this distribution is taken from the ratio of the intensity of the R head of the (0,0) band, 3060-3076Å, I_R, which is clearly distinguishable even under low resolution and when integrated over wavelength, to the intensity of the portion of the (0,0) from 3076 to 3120Å, I_0'. Under the assumption that the rotational distribution is thermal, the line strengths and fractional populations of the various levels can be combined to yield a functional relationship between the ratio I_R/I_0' and the rotational temperature. A measurement of the ratio then provides an estimate of the (thermal) rotational distribution without resolution of the individual lines in the spectrum. As a test, the application of this method to the $1 \rightarrow 0$ transfer data with D_2 as a fill gas gives a temperature of 850 ± 150°K as compared to 700 ± 50°K obtained from the

$Q_1 1$ - $Q_1 4$ ratios in the resolved spectra, so the method is reliable to within its inherent uncertainty. From all of the transfer data obtained with $v_i = 2$ and N_2 as the collision partner, an average ratio of $I_R/I_0' = 0.26 \pm 0.03$ is obtained to give a temperature of 1900 ± 500°K. Even with the large error limits, it is clear that higher rotational levels of $v_f = 0$ are being populated in this experiment than in the transfer from $v_i = 1$. Thus, as with the $1 \rightarrow 0$ transfer, some of the energy is being channeled into rotation of the OH. However, although the total amount is larger, the fraction going into rotation is about the same, between 20 and 25%, at least for N_2. (The actual N_f distribution resulting directly from $2 \rightarrow 0$ transfer is somewhat hotter than the quoted value, since a fraction of the observed distribution in $v_f = 0$ is caused by $1 \rightarrow 0$ transfer following $2 \rightarrow 1$ transfer, which results in a cooler overall temperature.)

Experimentally, the high temperature requires the consideration of the overlap of high N transitions of the (0,0) band with the (1,1) band to correctly relate the measured intensities to populations. Taking 3120Å as the operational separation point for the two bands (chosen because there is an easily recognizable break in the integrated spectrum at this point and no (1,1) lines occur below this wavelength), sums over the known transitions of v' = 0 weighted by their line strengths and fractional populations at 1900°K show that 15.6% of the (0,0) band emission is included in the measured (1,1) intensity. This leads to a 19% adjustment in the 'effective Einstein coefficients' for use in Eq. (1) for this experiment. This has little effect on the total transfer rate, from

Eq. (5), but would on the separately determined V_{21} and V_{20}. Again, the agreement expressed in Table 4 indicates that this adjustment has been properly made.

We conclude that this facet of the study is also in accord with the previously developed view. From the total transfer rate, which is assigned an uncertainty due only to the scatter in the data since it is nearly independent of the assumptions made concerning rotational distributions, it is seen that transfer out of $v_i = 2$ occurs at a rate not unlike that found for vibrational relaxation of $v_i = 1$, and varies similarly with initial rotational level. The uncertainties in the individual rates are larger, being a combination of both fitting errors and the estimated uncertainties in $\overline{V}_{10}$ and the overlap correction, but the results are still significant. Although the dependence of the transfer rate on initial rotational level is not clear from the values of V_{21} alone, it should be noted that any errors introduced by the assumptions will affect the results of both excitations equally so any comparisons need only consider the fitting error, and the plots in Fig. 7b are clearly divergent. The values for V_{20} also show the dependence on initial rotation, even with the large scatter in the data, so it can be said that, at least qualitatively, two-quantum transfer from $v_i = 2$ shows the same rotational dependence as single-quantum transfer from either $v_i = 2$ or 1. We feel that this clearly indicates that the N_i dependence of the vibrational transfer rates as a whole must be governed by some entrance channel dynamics, and cannot be ascribed to any kind of customary rate-versus- energy defect formulation.

DISCUSSION

Experimental Uncertainties

Errors in the experimental results are of two kinds. The first is due to scatter in the data, and is characterized by the confidence limits on the fitted parameters furnished by the least-squares routine. It is these confidence limits (1-σ level) which are listed in Tables 1, 3 and 4. They are the pertinent ones to consider when comparing different rates or cross-sections from this study, for example V_{10} as a function of N_i. Other possible errors entering into the determination of V_{21} and V_{20}, due to the need to calculate $\overline{V}_{10}$ and correct for some overlap of the bands, have been discussed in the Results section.

Uncertainties in the absolute rates or cross sections contain additional contributions from uncertainties in the pressure measurements, amplifier linearity, the value of the temperature chosen, the true lifetime, and the corrections (Appendix B) for background gas quenching. We estimate (see I for some discussion of these points) that the total contribution from these (uncorrelated) sources is about 10%, and combine that with the fitting errors to assign an overall typical absolute uncertainty of about 15%.

Other Investigations of Vibrational Transfer

There are three other reports of studies of vibrational relaxation in the $A^2\Sigma^+$ state of OH. Each of these uses tunable laser fluorescence pumping of individual N_i levels as in the present work. Only one, however,

was carried out using sufficient spectral resolution of the fluorescence such that vibrational transfer rates can be extracted.

Hogan and Davis[19] (HD) made lifetime measurements on fluorescence spectrally sorted with interference filters. A model of their experiment[20] using our previously reported V_{10} results[2] and their Q_0 values[19] showed that V_{10} and Q_1 cannot be extracted from their data; however the HD Q_0 values are not affected[14,20] by these considerations.

Killinger, Wang and Hanabusa[21] (KWH) have observed fluorescent spectra of the (0,0) and (1,1) bands under low ("16Å") resolution following excitation of $F_1(0)$ or $F_1(1)$ in $v_i = 1$. As KWH note, quantitative results cannot be obtained from their data. However, on the basis of a comparison of the intensities at 3145 and 3090Å as a function of N_2 pressure and for the two different pump levels, KWH claim that isoenergetic transfer makes an important (though not dominant) contribution, in contradiction to our findings using rotationally resolved fluorescence. Now rotational relaxation within $v_i = 1$ proceeds slowly enough compared to vibrational transfer that the (1,1) band should consist predominantly of emission from the initially excited level (our N_2 spectra appear very similar to that shown in Fig. 2c). The spectra emitted by $F_1(0)$ and $F_1(1)$ appear

[19] P. Hogan and D. D. Davis, "Electronic Quenching and Vibrational Relaxation of the OH($A^2\Sigma^+$,v'=1) state," J. Chem. Phys. 62, 4574-4576 (1975).

[20] R. K. Lengel and D. R. Crosley, "Comment on 'Electronic Quenching and Vibrational Relaxation of the OH($A^2\Sigma^+$, v'=1) State'," J. Chem. Phys. 64, 3900-3901 (1976).

[21] D. K. Killinger, C. C. Wang and M. Hanabusa, "Intensity and Pressure Dependence of Resonance Fluorescence of OH Induced by a Tunable uv Laser," Phys. Rev. 13, 2145-2152 (1976).

quite different, owing to the fact that only half the normal six branches are present in emission from the former while the latter lacks only one weak line. Under low resolution a maximum will appear for each in the 3135-3155Å region but the proportionality between population and intensity at 3145Å differs for the two levels. A full investigation of the discrepancy between the conclusions expressed in KWH and those found here for the existence of isoenergetic transfer would require a modelling study similar to that undertaken to understand the HD results, but we feel that the sparsity of quantitative results in the KWH work does not warrant such an undertaking. We finally remark that the use of our transfer and quenching rates to calculate a fluorescence efficiency for atmospheric pressure laser excitation measurements yields a value significantly lower than that used by Wang, Davis, and coworkers[22] to analyze data for such experiments. This has also been pointed out by German,[16] who mentions possible consequences of a different value of the efficiency.

German[13] has made intensity measurements of the type described here, together with lifetime measurements on fluorescence spectrally sorted by a low-resolution (35Å bandpass) spectrometer. Vibrational transfer rates V_{10} for the V'=1 level were obtained from the intensity data, the quench rate Q_0 was determined from lifetimes, and the combination furnished Q_1. For the V'=2 level, quench rates could not be determined but intensity measurements yielded V_{21} and V_{20}.

[22] C. C. Wang and L. I. Davis, Jr., "Measurement of Hydroxyl Concentrations in Air Using a Tunable uv Laser Beam," Phys. Rev. Letters 32, 349-352 (1974); C. C. Wang, L. I. Davis, Jr., C. H. Wu, S. Japar, H. Niki and B. Weinstock, "Hydroxyl Radical Concentration Measured in Ambient Air," Science 189, 797-800 (1975); C. C. Wang, L. I. Davis. Jr., C. H. Wu and S. Japar, "Laser Induced Dissociation of Ozone and Resonance Fluorescence of OH in Ambient Air," Appl. Phys. Lett. 28, 14-16 (1976).

German's results for V_{10} and Q_0 using H_2 and N_2 as well as V_{21} and V_{20} for N_2, are compared with ours in Table 5 (he also investigated O_2 as a collision partner, and V_{21} and V_{20} in OD). German separately measured Q_0 for N_i = 1,4 and 5 in v_i = 1, for both H_2 and N_2. Those results are independent of N_i, as we expected in our use of Eq. (2). The average of his Q_0 determinations is listed. Our entries for V_{10} in OD, N_i = 1, are obtained from the relationship $V_{10}^{OD}(1) = V_{10}^{OD}(0)V_{10}^{OH}(1)/V_{10}^{OH}(0)$. This is not fully correct, but reasonable, since our measured value of $V_{10}^{OD}(0)$ is likely a bit low, due to rotational averaging, whereas the $V_{10}(1)/V_{10}(0)$ ratio is probably a little closer to unity in OD than in OH, as discussed in the results section. The only values which disagree significantly between German's work and our own are the quench rates Q_0, which are discussed below, and the relative rates of one- and two-quantum transfer from v_i = 2.

German's results for V_{21} and for the total rate of transfer out of v_i = 2 in OH agree with ours within an overlap of error bars, but the results for V_{20} do not. In particular, he finds that V_{21} and V_{20} are the same (within experimental uncertainty) while we find a ratio of 1.4 ± 0.2 (it should be noted that our preliminary value of 1.7 for this ratio, quoted earlier,[7c] was too high). German gives no details concerning his spectral resolution in this portion of the experiment; in addition he estimates $\overline{V}_{10}$ as $1.1V_{10}(N_i = 1)$, which is some 50% higher than the value we used considering the rotational distribution to be the same as in 1 → 0 transfer. This would affect the ratio of the two rates, but not the total, and on that basis we feel our values are

TABLE 5. COMPARISON OF CROSS SECTIONS ($Å^2$) MEASURED BY GERMAN (REF. 17) WITH OURS. SEE TEXT FOR FURTHER DETAILS CONCERNING FOOTNOTES.

ISOTOPE	COLLISION PARTNER	CROSS SECTION	N_i	GERMAN, REF. 17	PRESENT WORK
OH	H_2	σ_{10}	1	9.7±0.7	9.2±0.5
			4	6.5±0.5	6.8±0.3
		σ_{Q0}	-	7.0±0.6[a]	4.6±0.5
	N_2	σ_{10}	1	19.6±1.1	23.0±1.2
			4	12±1.1	17.1±0.9
		σ_{Q0}	-	3.4±0.3[a]	5.8±0.7
		σ_{21}		17±2	14.8±1.2
		σ_{20}		15±3	10.7±1.2
		$\sigma_{2,total}$[b]		32±5	25.5±1.7
OD	H_2	σ_{10}	1	9.8±0.7	8.2±0.6[c]
		σ_{Q0}	-	7.9±0.7[d]	6.3±0.8
	N_2	σ_{10}	1	17.5±1.2	14.8±0.5[c]
		σ_{Q0}	-	3.5±0.5[e]	4.4±0.5

[a]Average for three values of N_i = 1,4 and 5.

[b]The sum of German's σ_{21} + σ_{20}, and our separately determined total.

[c]Scaled from OD results and OH ratios.

[d]Average for N_i = 1 and 2.

[e]Obtained with N_i = 1.

preferable. While we have no direct experimental comparison with German's transfer rates from $v_i = 2$ in OD, we are somewhat suspicious of his large ratio $V_{21}/V_{20} = 4$ for N_2, noting that again the sum of the rates is the same as in OH, as might be expected from our mechanistic viewpoint and analogy to $v_i = 1$ transfer in the two isotopes, taken together with concerns about his value of $\overline{V}_{10}$.

In summary, however, it should be remarked that the entries in Table 5 represent, for the most part, excellent agreement in the field of energy transfer measurements, for absolute values obtained in two separate laboratories.

Quenching Rates

We have treated the quenching entirely as a parameter which enters into the overall form of the observed data; see Eq. 4. That is, we have made no separate attempts to measure it independently, in the normal way through the pressure dependence of the total fluorescence or the lifetime from time-domain measurements. In fact, the plots such as in Fig. 3 and our non-linear, 4-parameter fits represent a different method of obtaining Q_0 than has been used previously. Consequently our results for this quantity form a most useful adjunct to the more customary techniques of measuring it. However, our results are clearly correlated with our values for V_{10} obtained from the same fits, so we do not claim any preference for our values over the more direct determinations.

For each of our major series of measurements (OH with H_2, D_2 and N_2; OD with H_2 and N_2) we carried out not only the four-parameter fit described above but also fitted the data for each N_i separately to a $V_{10}(N_i)$ and $Q_0(N_i)$.* In each case we found the same values of $V_{10}(N_i)$ as in the four-parameter fit, and the values obtained for the $Q_0(N_i)$ were identical as well as the same as the reported Q_0, when the data-fitting error bars are taken into account. The only difference was that here the error bars were somewhat larger, especially for the quench rates; this reflects the fact that in the separate fits there are fewer data points per fitted parameter.

Schofield[8] has summarized, in the form of a table and a graph, and with some comment, determinations of the values of Q_0 for a number of different gases. Besides our own, there exist four other experiments utilizing laser induced fluorescence from a single level; each of these (unlike ours) obtains Q_0 from the effect of added pressure on the radiative lifetime measured in a time-domain experiment. The Brophy *et al.*[23] cross section for H_2 assumes that all of the quenching in that experiment is due to that gas, and none was caused by NO_2; our finding of a large quench rate for NO_2 (Appendix B) causes us to view their relatively large cross section** of 13Å² with some suspicion. Becker *et al.*[24] find a value** of 4.3 ± 0.6Å² for $\sigma_{10}(H_2)$, in good agreement with our own findings. On

*This notation is not meant to imply a functional form of physical significance, but merely a mathematical connection in the data-fitting sense.

[23] J. H. Brophy, J. A. Silver and J. L. Kinsey, "Direct Measurement of the Radiative Lifetime of the $A^2\Sigma^+$ (v'=0, K'=1, J'=3/2) State of OH and OD," Chem. Phys. Letters 28, 418-421 (1974).

[24] K. H. Becker, D. Haaks, and T. Tatarczyk, "The Natural Lifetime of $OH(^2\Sigma^+$, v=0, N=2, J=3/2) and its Quenching by Atomic Hydrogen," Chem. Phys. Letters 25, 564-567 (1974).

**Adjusted from the lifetime used in their data analysis to the value of 0.7 μsec.

the other hand, the HD results[14] and those of German[13] are in good agreement with one another; the HD values for H_2 and N_2 are, respectively, 7.4 ± 1.0 and $3.8 \pm 0.4 Å^2$, while German's are listed in Table 5.

We find disturbing the lack of agreement of our values for the H_2 and N_2 quench rates for OH with those of German, in view of the good agreement for the other quantities expressed in Table 5. In addition, our rates for OD quenched by H_2 and N_2 show an ordering opposite to our findings for OH, but in agreement with German. We take solace in the agreement with the Becker *et al.* result, but do not understand the overall discrepancy. (It should be noted, for example by comparing the spread of points in Ref. 8, that in the overall history of the OH A-state, all four experiments would normally be considered to be in agreement.) There is no ambiguity in the fact that our reported results for Q_0 are those which do fit the data, and the agreement between two different kinds of experiments (those of Ref. 24 and ours) has some intrinsic merit. However, the values of σ_{Q0} for H_2 and N_2 must still be considered an open question; we cannot definitively recommend our values over those of German or HD.

Conclusions

In general, the smooth variation of our measured rates with incident and final quantum level (see also III) and the good agreement of German's findings[13] with our own gives us confidence in our results, even on an absolute basis. (It is our contention that this good agreement is a consequence of the manner in which the experiments were carried out, that is, a clean selection of the initial level using laser excitation, and a

definitive detection of the final level of the energy transfer processes using fluorescence dispersed by a spectrometer). In turn, we feel justified in drawing from these results mechanistic inferences, and recommending their use in other studies, e.g., in models of reaction networks incorporating energy transfer.

From the standpoint of practical worth, the results presented here provide not only a generally useful set of parameters for data reduction in a variety of experiments, but point to some specific areas of consideration. In studies of processes that produce the A state directly, such as combustion and photochemical reactions, conclusions based on measured state distributions, both rotational and vibrational, must take into account the relaxation rates of the OH. For example, it cannot, except at high pressures, be assumed that there is a thermal equilibrium between translation, rotation, and vibration; any process that selectively produces the OH in $v' = 1$, or higher, can show a thermal rotational distribution in $v' = 0$ that is not directly related to the translational temperature, nearly equal vibrational populations, and a rotational distribution in the initial vibrational level that is little changed from the nascent distribution. It must also be realized that the rotational dependence of the vibrational transfer rate can cause alterations in the populations of the upper vibrational levels; an initially thermal distribution in $v' = 1$ will be rotationally "heated" by the faster removal of lower rotational levels. The detailed transfer rates, both rotational and vibrational, must also be used in those experiments probing ground state OH concentrations by laser induced fluorescence. For atmospheric

measurements, it is common practice to excite the OH to v' = 1 and observe the fluorescence from transferred v' = 0 molecules; changing the wavelength of excitation by as little as 0.7Å ($P_1 1$ and $Q_1 3$ absorptions in the (1,0) band) can change the yield of v' = 0 fluorescence and thus results for populations uncorrected for transfer rate variations, by twenty percent. Attention must also be paid in such intensity of transferred fluorescence measurements to the spectral response of the detector system and how it is related to the rotational and hence wavelength distribution of the fluorescence.

Conjectures concerning the mechanism by which the vibrational transfer takes place have been liberally sprinkled throughout the text, and are here briefly summarized. The central idea is that the overall collision process is dominated by a strong, anisotropic, attractive potential of interaction between the OH and its collision partner. This potential leads to a long lived collision, which cannot be specified as being due to either an actual complex formation, an orbiting collision, or a simple reduction in relative velocity. For vibrationally excited OH, this long lived collision leads to a close coupling process in which the excess energy is partitioned among all degrees of freedom of the collision pair, and a partner that lacks internal degrees of freedom is inefficient in absorbing the energy and hence causing transfer. Since all energetically accessible modes are available for excitation during a long lived collision, there is no propensity for isoenergetic transfer, and the high energy defect process of transferring two quanta of OH vibrational energy is made relatively efficient. The strength of this attractive potential,

and thus its effectiveness in giving rise to a long lived collision, is dependent upon the orientation of the OH with respect to the incoming collision partner, and this orientation is in turn time dependent because of both the relative motion of the colliding molecules and the rotation of the OH. As the speed of the OH rotation increases, the potential is effectively decreased and the probability of having a collision that is conducive to vibrational energy transfer is lessened. We contend that all of the experimental results (with the possible exception of the increase in the temperature, of the N_f distribution following $1 \rightarrow 0$ transfer, with complexity of the collision partner) are in accord with this simple picture. A further systematization and some comparison with the rotational transfer findings are carried out in III using the techniques of information theoretic analysis.

ACKNOWLEDGEMENT

We gratefully acknowledge the National Science Foundation for their support of the portion of this work carried out while both authors were at the University of Wisconsin.

REFERENCES

1. See, e.g., "State-to-State Chemistry," ACS Symposium Series 56 (1977).

2. R. K. Lengel and D. R. Crosley, "Rotational Dependence of Vibrational Relaxation in $A^2\Sigma^+$ OH," Chem. Phys. Lett. 32, 261-264 (1975).

3. R. K. Lengel and D. R. Crosley, "Energy Transfer in $A^2\Sigma^+$ OH. I. Rotational," J. Chem. Phys. 67, 2085-2101 (1977).

4. R. K. Lengel and D. R. Crosley, "Energy Transfer in $A^2\Sigma^+$ OH. III. Surprisal Analysis," to be published.

5. R. D. Levine and R. B. Bernstein, "Energy Disposal and Energy Consumption in Elementary Chemical Reactions; The Information Theoretic Approach," Acct. Chem. Res. 7, 393-400 (1974).

6. R. K. Lengel, "Energy Transfer in $A^2\Sigma^+$ OH," Ph.D. Thesis, University of Wisconsin, Madison, WI, June 1976.

7. R. K. Lengel and D. R. Crosley, (a) "Collisionally Induced Energy Transfer in the $A^2\Sigma^+$ of OH," Bull. Amer. Phys. Soc. 19, 154 (1974); (b) "Vibrational Relaxation in the $A^2\Sigma^+$ State of OH," Paper FD6, Symposium on Molecular Spectroscopy, Columbus, Ohio, June 1974; (c) "Energy Transfer Studies on $A^2\Sigma^+$ OH Using Tunable Laser Excitation," Paper TH6, Sumposium on Molecular Spectroscopy, Columbus, Ohio, June 1975; (d) "Energy Transfer in $A^2\Sigma^+$ OH," Paper TC1, Symposium on Molecular Spectroscopy, Columbus, Ohio, June 1976; (e) "State-to-State Relaxation in $A^2\Sigma^+$ OH and OD," in Ref. 1.

8. K. Schofield, "Critically Evaluated Chemical Kinetic Rate Constants for Gaseous Reactions of Electronically Excited Species," J. Phys. Chem. Ref. Data, in press.

9. The rotational branch terminology is that normally employed for OH; see G. H. Dieke and H. M. Crosswhite, "The Ultraviolet Bands of OH," Johns Hopkins University Bumblebee Report No. 87 (1948), republished in J. Quant. Spectrosc. Radiat. Transfer 2, 97-199 (1962).

10. D. R. Crosley and R. K. Lengel, "Relative Transition Probabilities and the Electronic Transition Moment in the A-X System of OH," J. Quant. Spectrosc. Radiat. Transfer 15, 579-591 (1975).

11. D. R. Crosley and R. K. Lengel," Relative Transition Probabilities in the A-X System of OD," J. Quant. Spectrosc. Radiat. Transfer 17, 59-71 (1977).

12. D. R. Crosley, "Level Crossings and Anisotropic Emission in a $^2\Sigma$ - $^2\Pi$ Transition," BRL Report (to be published).

13. K. R. German, "Collision and Quenching Cross Sections in the $A^2\Sigma^+$ State of OH and OD," J. Chem. Phys. 64, 4065-4068 (1976).

14. P. Hogan and D. D. Davis, "Comments on 'Electronic Quenching and Vibrational Relaxation of the OH ($A^2\Sigma^+$, v'=1) State'," J. Chem. Phys. 64, 3901 (1976).

15. G. C. Berend and R. L. Thommarson, "Vibrational Relaxation of HF and DF," J. Chem. Phys. 58, 3203-3208 (1973).

16. J. F. Bott, "HF Vibrational Relaxation Measurements Using the Combined Shock-tube-laser-induced Fluorescence Technique," J. Chem. Phys. 57, 96-102 (1972).

17. J. F. Bott, "Vibrational Relaxation of HF(v-1) and DF(v-1) by H_2 and D_2," J. Chem. Phys. 61, 2530-2535 (1974).

18. K. R. German, "Direct Measurement of the Radiative Lifetimes of the $A^2\Sigma^+$(v=0) States of OH and OD," J. Chem. Phys. 62, 2584-2587 (1975).

19. P. Hogan and D. D. Davis, "Electronic Quenching and Vibrational Relaxation of the OH($A^2\Sigma^+$,v'=1) state," J. Chem. Phys. 62, 4574-4576 (1975).

20. R. K. Lengel and D. R. Crosley, "Comment on 'Electronic Quenching and Vibrational Relaxation of the OH($A^2\Sigma^+$, v'=1) State'," J. Chem. Phys. 64, 3900-3901 (1976).

21. D. K. Killinger, C. C. Wang and M. Hanabusa, "Intensity and Pressure Dependence of Resonance Fluorescence of OH Induced by a Tunable uv Laser," Phys. Rev. 13, 2145-2152 (1976).

22. C. C. Wang and L. I. Davis, Jr., "Measurement of Hydroxyl Concentrations in Air Using a Tunable uv Laser Beam," Phys. Rev. Letters 32, 349-352 (1974); C. C. Wang, L. I. Davis, Jr., C. H. Wu, S. Japar, H. Niki and B. Weinstock, "Hydroxyl Radical Concentration Measured in Ambient Air," Science 189, 797-800 (1975); C. C. Wang, L. I. Davis. Jr., C. H. Wu and S. Japar, "Laser Induced Dissociation of Ozone and Resonance Fluorescence of OH in Ambient Air," Appl. Phys. Lett. 28, 14-16 (1976).

23. J. H. Brophy, J. A. Silver and J. L. Kinsey, "Direct Measurement of the Radiative Lifetime of the $A^2\Sigma^+$ (v'=0, K'=1, J'=3/2) State of OH and OD," Chem. Phys. Letters 28, 418-421 (1974).

24. K. H. Becker, D. Haaks, and T. Tatarczyk, "The Natural Lifetime of OH($^2\Sigma^+$, v=0, N=2, J=3/2) and its Quenching by Atomic Hydrogen," Chem. Phys. Letters 25, 564-567 (1974).

25. The pressures quoted in Appendix B refer to pressures measured downstream from the reaction region (see I) under conditions in which the microwave discharge was off and no reaction took place. Our Alphatron gauge readings are corrected to "true" pressures using the results of R. Holanda (Investigation of the Sensitivity of Ionization-type Vacuum Gauges," J. Vac. Sci. Tech. 10, 1133-1139 (1973), and private communication). We do not know if they correspond to the actual pressures of these gases under conditions in which the OH is produced.

26. A. McKenzie, M. F. R. Mulcahy and J. R. Steven, "Reaction Between Hydrogen Atoms and Nitrogen Dioxide," J. Chem. Soc. Far. Trans. I, 70, 549-559 (1974).

27. J. H. Brophy, J. A. Silver, and J. L. Kinsey, "Vibrationally Excited OH^+ from the Reaction of H with NO_2 Observed by Laser-induced Fluorescence," J. Chem. Phys. 62, 3820-3822 (1975).

APPENDIX A. THE TIME-DEPENDENT EQUATIONS

It has been pointed out (see I) that a steady-state situation is not fully appropriate to the experimental conditions. In Appendix A to I it was demonstrated in a general fashion that the signals resulting from an integral of the intensities over all time (in our stretching preamplifier) obeyed equations identical to those obtained from the steady state equations. We here explicitly integrate the time dependent equations for the two-level system:

$$dN_1/dt = Z \exp(-Lt) - D_1 N_1$$

$$dN_0/dt = V_{10} N_1 - D_0 N_0.$$

Here the laser pulse is described (adequately) by an exponential falloff at a rate L following an initial sharp turn-on; Z contains the laser flux, ground state OH density and absorption coefficient; $D_1 = 1 + (V_{10} + Q_1)P$; $D_0 = 1 + Q_0 P$; $\tau_0 = \tau_1 = 1$. These equations are solved in a straightforward fashion to yield $N_1(t)$ and $N_0(t)$ as sums of exponentials:

$$N_1(t) = Z(L - D_1)^{-1}(\exp(-D_1 t) - \exp(-Lt)) \qquad (A1)$$

$$N_0(t) = ZV_{10}(L - D_1)^{-1}((L - D_0)^{-1}\exp(-Lt) - (D_1 - D_0)^{-1}\exp(-D_1 t) + (L - D_1)(L - D_0)^{-1}(D_1 - D_0)^{-1}\exp(-D_0 t)) \qquad (A2)$$

Such a combination was observed (qualitatively) in the time domain experiments made to verify, in part, that the N_f distribution of Fig. 5 is the nascent, single collision result. The quantitative intensity data was taken, however, with a preamp having a measured time constant

F^{-1} = 23 μsec, significantly larger than any of the characteristic times D_1^{-1} and D_0^{-1} of the signal. L^{-1} was shorter, less than 140 nsec. These stretched signals were then fed into the boxcar and detected with a gate open from t = 1 to t = 14 μsec following the laser pulse. Equations A1 and A2 are first integrated to yield the voltage responses $E_1(t)$ and $E_0(t)$ of the simple RC circuit for which $N_1(t)$ and $N_0(t)$ represent the input voltages. At long times, these results are dominated by the RC-stretched exponential term. For example, at t = 6.5 μsec,

$$E_1(t) = ZF(D_1 - F)^{-1}(L - F)^{-1} \exp(-Ft)$$

$$E_0(t) = ZFV_{10}(D_1 - F)^{-1}(D_0 - F)^{-1}(L - F)^{-1} \exp(-Ft)$$

describes the results to within 0.1%. Thus the ratio $\int_1^{14} E_0(t)dt / \int_1^{14} E_1(t)dt$ is the same as the steady state ratio in Eq. (4), N_0/N_1, except that the denominator is now $D_0 = 1 + Q_0P - F = 0.97 + Q_0P$ instead of $1 + Q_0P$ alone.

The application of a similar approach to the 15 time dependent populations appropriate to the rotational transfer in I yields the same 3% correction. This is because the stretched time-dependent signals are there again a sum of exponentials which at long times is dominated by the exp(- Ft) term.

APPENDIX B. BACKGROUND GAS COLLISIONS

It is clear from Figs. 2 and 3 that some vibrational transfer occurs due to collisions with the background gases H_2O and NO_2. This is easily corrected for, as described in the text, by measurements at zero fill gas pressure. Somewhat more difficult is the correction for quenching.

Due to these problems, the flow rates (as determined by measured pressures and controlled by needle valves) of the reactants are maintained at the same constant value for all experimental runs. During one phase of this research, considerable effort was expended in an attempt to characterize and understand the effects of the pressure of the reactants on the production of ground state OH within our system. The characterization was achieved but the understanding was not. A pressure[25] of 6 mtorr H_2O was chosen as a compromise between discharge stability, signal intensity, and pressure stability (this last becomes a factor at high flow rates due to evaporative cooling of the H_2O reservoir). At this water pressure, the fluorescence signal increases nearly linearly with NO_2 pressure up to 8 mtorr, becomes almost constant in the 8-13 mtorr region, and decreases rapidly beyond 17 mtorr of NO_2. Except for a slower

[25] The pressures quoted in Appendix B refer to pressures measured downstream from the reaction region (see I) under conditions in which the microwave discharge was off and no reaction took place. Our Alphatron gauge readings are corrected to "true" pressures using the results of R. Holanda (Investigation of the Sensitivity of Ionization-type Vacuum Gauges," J. Vac. Sci. Tech. 10, 1133-1139 (1973), and private communication). We do not know if they correspond to the actual pressures of these gases under conditions in which the OH is produced.

initial increase, our data is not unlike that shown in Fig. 5 of Ref. 26. A final working pressure of 11 mtorr NO_2 is chosen; our observations suggest that there is very little undissociated H_2O remaining in the OH production region.

Maintenance of the NO_2 pressure at a constant value assures the reproducibility of the results; however, a numerical value is needed in order to obtain absolute rates (not relative ones). Due to the fact that the NO_2 pressure also affects the concentration of ground state OH and hence the overall fluorescence signal, direct measurement of $Q(NO_2)$ through a decrease in fluorescent intensity was not possible. Instead, we rewrite the steady state expression to explicitly include the NO_2 quenching and rearrange to obtain

$$N_1/N_0 = (1 + QP)/V_{10}P + Q(NO_2)P(NO_2)/V_{10}P.$$

The ratio N_1/N_0 has been measured for a series of NO_2 pressures with H_2 fill gas pressures of 0.16 and 0.32 torr. The resulting linear plots give slope to intercept ratios of $Q(NO_2)/(1 + QP)$. The value for the H_2 quench rate was taken from the fits to the relative populations versus H_2 pressure, under the assumption of no NO_2 quenching, and used to find an initial value of $Q(NO_2)$. This value of $Q(NO_2)$ is then used to obtain an improved value of Q for H_2 and hence an improved $Q(NO_2)$, which was within experimental error of the first value. The result is that $Q(NO_2) = 23 \pm 3$ torr$^{-1}\tau^{-1}$, corresponding to a cross section of 150 ± 20Å^2.

[26] A. McKenzie, M. F. R. Mulcahy and J. R. Steven, "Reaction Between Hydrogen Atoms and Nitrogen Dioxide," J. Chem. Soc. Far. Trans. I, 70, 549-559 (1974).

At our working pressure, this amounts to a 26% shortening of the lifetime; while the NO_2 quench rate has not been well determined, the error in this correction amounts to about an overall 3% contribution to the error in the absolute rates. This is the largest contribution outside the fitting error.

From lifetime measurements at lower pressures, German[18] has obtained a value of the NO_2 quench rate which is only about a third of that found here. We do not understand the discrepancy. However, since we do not know that actual pressure of NO_2 under conditions in which the H_2O is dissociated, our "working value" of the NO_2 quenching which was obtained under the actual operating conditions forms, we feel, a more self-consistent correction to our energy transfer data than the use of his value and an estimate of our NO_2 pressure. That is, we have much more faith in our correction than in the accuracy of $Q(NO_2)$ on any absolute basis.

APPENDIX C. STIMULATED EMISSION

At the laser power used, stimulated emission can occur in the exciting transition at a rate competitive with spontaneous emission. It is necessary[27] to inquire as to whether this alters the effective branching ratios used in Eq. (1) or the line strengths needed for analysis of the rotational transfer data in I. We here demonstrate that the long OH lifetime, compared to the laser pulse length, makes such effects negligible in our experiment.

A two-state system with a time-dependent upper state population N_u and a time-independent total population N_0 is described by

$$dN_u/dt = B\bar{I}(N_0 - N_u) - BI_0N_u - AN_u. \qquad (A3)$$

Here B and A are Einstein coefficients and $\bar{I}$ is the time-dependent laser power, $\bar{I} = I_0 \exp(- Lt)$, as in Appendix A. We set $C = I_0 B N_0$ and $K = 2 I_0 B$, so that Eq. (A3) reads

$$dN_u/dt = (C - KN_u)\exp(- Lt) - AN_u$$

This has the formal solution

$$N_u = \exp[f(t)]\int_0^t C \exp[- sL - f(s)]ds$$

or the series solution

$$N_u = (C/A)\exp[f(t)]\{\sum_n Q_n \exp(- K/L) + \sum_n Q_n \exp[- (n + 1)lt]\} \qquad (A4)$$

Here, $f(t) = At + \exp(- Lt)$

and $Q_n = (K/A)^2[(1 - L/A)\ldots(1 - (n + 1)L/A)]^{-1}$.

[27] J. H. Brophy, J. A. Silver, and J. L. Kinsey, "Vibrationally Excited OH^+ from the Reaction of H with NO_2 Observed by Laser-induced Fluorescence," J. Chem. Phys. 62, 3820-3822 (1975).

In the region of the (0,0) band for example, $B/A = 7.4 \times 10^{8}$ $(\text{watt/cm}^2\ \text{Hz})^{-1}$ for the two-level system. Now OH is not a two-level system; rather the pumping transition (e.g., $Q_1 3$) is only one of six rotational branches which are spontaneously emitted. We account for this by multiplying the above B/A by the fraction of the intensity (0.395) contained in the $Q_1 3$ branch.* The value of I_0 is obtained from the measured average power (0.5 mW) in the ultraviolet, the beam area at the excitation region, which is estimated visually as 0.02 cm^2, the laser duty factor (10^{-5}), and the laser linewidth, measured as 4 cm^{-1} full width at half maximum. Now the OH linewidth is smaller (0.1 cm^{-1}) so we take the spectral power density at the peak, corresponding to optimum tuning. Dividing by 4π since laser is not isotropic yields $I_0 = 1.6 \times 10^{-19}$ watt $\text{cm}^{-2}\text{Hz}^{-1}$. Consequently $BI_0/A = 0.45$, so that stimulated emission is of importance during the laser on-time, which is characterized by the measured** $L/A \leq 5$. These values form the input to the model, Eq. (A4), and are compared to the value for $BI_0 = 0$ (no stimulated emission). Truncation of (A4) is made after n = 4, which yields a remainder of $< 10^{-6}$. Plots[6] of the model calculations show that N_u peaks at the same time ($0.4\ A^{-1}$) for $B = 0$ and $B \neq 0$, and that for times $> 0.9\ A^{-1}$ the curves are indistinguishable. The stimulated emission is

*This value is appropriate to pumping in (0,0). For pumping in (1,0), the fraction is smaller (0.232) since there is spontaneous emission in (1,1) as well. We are thus here considering the case in which stimulated emission is the most important.

**This is actually the time dependence of the fundamental (visible) dye laser pulse. We expect that the non-linear character of the frequency doubling will shorten the ultraviolet pulse, so that this represents an upper limit. Our actual estimate is L/A = 8.

hence unimportant for our energy transfer experiments in which the signal is integrated and gated (Appendix A). In general, the effectiveness of the large value of BI_0/A is offset by the large value of L/A, that is, stimulated emission causes problems only when the laser is of high power and has a pulse length matching the radiative lifetime.

DISTRIBUTION LIST

No. of Copies	Organization
12	Commander Defense Documentation Center ATTN: DDC-TCA Cameron Station Alexandria, VA 22314
1	Commander US Army Materiel Development and Readiness Command ATTN: DRCDMD-ST, N. Klein 5001 Eisenhower Avenue Alexandria, VA 22333
1	Commander US Army Aviation Research and Development Command ATTN: DRSAV-E P.O. Box 209 St. Louis, MO 63166
1	Director US Army Air Mobility Research and Development Laboratory Ames Research Center Moffett Field, CA 94035
1	Commander US Army Electronics Research and Development Command Technical Support Activity ATTN: DELSD-L Fort Monmouth, NJ 07703
1	Commander US Army Communications Rsch and Development Command ATTN: DRDCO-PPA-SA Fort Monmouth, NJ 07703
1	Commander US Army Missile Research and Development Command ATTN: DRDMI-R Redstone Arsenal, AL 35809
1	Commander US Army Missile Materiel Readiness Command ATTN: DRSMI-AOM Redstone Arsenal, AL 35809
1	Commander US Army Tank Automotive Research & Development Command ATTN: DRDTA-UL Warren, MI 48090
5	Commander US Army Armament Research and Development Command ATTN: DRDAR-TSS (2 cys) DRDAR-LC, Dr. J. Lannon Dr. R. Field Dr. R. Harris Dover, NJ 07801
1	Director US Army TRADOC Systems Analysis Agency ATTN: ATAA-SL, Tech Lib White Sands Missile Range NM 88002
1	Purdue University Department of Chemistry ATTN: Dr. R. K. Lengel Lafayette, IN 47907
	Aberdeen Proving Ground
	Dir, USAMSAA Cdr, USATECOM ATTN: DRSTE-SG-H